ENGINEERING PROGRESS
at the
University of Florida

Vol. XVI, No. 2 February, 1962

TECHNICAL PAPER NO. 220

An Experimental Study of the Development of Cohesion and Friction with Axial Strain in Saturated Cohesive Soils

by

J. H. Schmertmann and J. O. Osterberg

Reprinted courtesy of the Soil Mechanics and Foundations Division of the American Society of Civil Engineers from *Research Conference on Shear Strength of Cohensive Soils*, University of Colorado, Boulder, Colorado, June, 1960.

Published monthly by the

FLORIDA ENGINEERING AND INDUSTRIAL EXPERIMENT STATION

COLLEGE OF ENGINEERING UNIVERSITY OF FLORIDA GAINESVILLE

Entered as second-class matter at the Post Office at Gainesville, Florida

AN EXPERIMENTAL STUDY OF THE DEVELOPMENT OF COHESION AND FRICTION WITH AXIAL STRAIN IN SATURATED COHESIVE SOILS

By John H. Schmertmann,[1] A. M. ASCE, and Jorj O. Osterberg,[2] F. ASCE

SYNOPSIS

Soil strength, at any strain, is divided into the components of cohesion and friction, with these redefined according to the changes in compressive strength associated with changes in intergranular stress while soil structure is held approximately constant. This paper reports the development of a triaxial compression test, herein called the CFS-test, designed to permit the computation of this cohesion and friction at strain intervals during compression and thereby permit the fitting of curves of the variation of cohesion and friction with strain.

In the most advanced stage of the CFS-test reported herein the specimen develops an axial deviator stress from the imposition of a constant rate of compressive strain. During this strain the pore water pressure is varied to maintain a constant, pre-selected value of $\bar{\sigma}_1$. Deviator stress vs. strain data are obtained during strain at this $\bar{\sigma}_1$, after which the pore pressure is changed to maintain a new constant value of $\bar{\sigma}_1$. Data are then obtained at this value of $\bar{\sigma}_1$. This procedure of alternating between the two chosen values of $\bar{\sigma}_1$ permits the fitting of two stress vs. strain curves—one for each $\bar{\sigma}_1$. These curves are then mathematically interpreted to obtain the defined cohesion and friction as a function of strain. The test is performed using only a single specimen, thus permitting the testing of natural soils.

Results are presented from the performance of CFS-tests on a variety of machine extruded and undisturbed, saturated, normally consolidated clay specimens. Within the limitations of the experimental program used in this research it is shown that:

1. The Coulomb-Hvorslev failure criteria equation is valid at any strain.
2. The measured cohesion and friction strength components act independently, with the maximum cohesion developing at much lower strains than the maximum friction.
3. The cohesion can have a pronounced "peaking effect."
4. The cohesion of a clay at a given water content is not a constant but is greatly dependent on soil structure.
5. At a given preconsolidation stress all clays tested had about the same value of maximum cohesion.
6. The maximum friction angle does not vary with preconsolidation stress in a consistent manner.

1. Asst. Prof. of Civ. Engrg., Univ. of Florida, Gainesville, Fla.
2. Prof. of Civ. Engrg., Northwestern Univ., Evanston, Ill.

I. INTRODUCTION

Notation.--The letter symbols adopted for use in this paper are defined and arranged alphabetically, for convenience of reference, in Appendix I.

Historical Review

The shear strength of clays has been a subject of discussion and disagreement ever since investigators began to think seriously about the subject. Most present day concepts spring from Coulomb's original equation; here expressed in the form $\tau_f = c + \sigma_f \tan \phi$, where τ_f is the maximum shear resistance, c is the cohesion and $\sigma_f \tan \phi$ is the friction on the failure plane on which the normal stress is σ_f. It was thought that c and ϕ were constant for a given soil and could be determined by simple tests. Early investigators using direct shear apparatus found that the test results were greatly influenced by the rate of shearing and by the initial water content of a given soil.

A. Casagrande pointed out that due to shearing a pore water pressure occurs and that the normal stress σ should be replaced by the intergranular stress $\bar{\sigma}$, where $\bar{\sigma} = \sigma - u$ and where u is the pore water pressure. (The writers have chosen to use the words intergranular stress in this paper instead of the more common effective stress because the former is considered less ambiguous and more descriptive.) Hvorslev (1)[3] by means of a large number of direct shear tests, drained and undrained, made on remolded specimens starting with remolded clay at the liquid limit and consolidating to different pressures before testing, modified Coulomb's expression: $s = \bar{c} + \bar{\sigma} \tan \bar{\phi}$ where $\bar{c}$ represents the effective cohesion and $\bar{\phi}$ the effective angle of internal friction. He concluded that c for a given soil is a function primarily of water content.

Simultaneously with Hvorslev's work, Terzaghi recognized the importance of the pore water pressure and volume change during testing. Triaxial tests showed that the Mohr failure envelope for unconsolidated undrained tests was a horizontal line since no volume and intergranular stress change occurred, and its intercept on the ordinate axis represented the undrained shear strength. Consolidated undrained and consolidated drained envelopes represented different volume changes and different intergranular stresses at failure. Since the consolidated drained tests represented a condition of negligible pore water pressure and all the stresses were essentially intergranular, the angle whose tangent was the slope of the Mohr envelope was sometimes thought to be the angle of internal friction. The critics of this approach point out that each Mohr circle represented a test result with the soil at a different water content, and the envelope therefore did not represent comparative tests on the same material.

Rutledge, on the basis of a large number of tests on clays made by a number of investigators, showed that the strength of a clay was a function of the water content at failure and independent of the pore water pressure or test method (2). He further showed that for the maximum $(\sigma_1 - \sigma_3)$ value, the water content vs. log $(\sigma_1 - \sigma_3)$ plotted a curve which was either a straight line or close to a straight line. In addition, he demonstrated that this strength curve was nearly parallel to the water content - log consolidation pressure $(\bar{\sigma}_1)$ curve. It was assumed that the water content-consolidation curve was a

3. Numerals in parentheses refer to corresponding items in Appendix II--References.

unique curve, being only a function of $\bar{\sigma}_1$ and independent of the magnitude of the minor and intermediate principal stresses. Rutledge stated ". . . there is doubt that saturated cohesive soils can be considered to have an angle of internal friction." The data on which Rutledge based his conclusions were from tests on undisturbed specimens of naturally deposited saturated clays which were normally or nearly normally consolidated.

Bjerrum showed that for normally consolidated clays the water content-consolidation pressure relationship was independent of the minor and intermediate principal stresses but that for other clays it was not (3). Pore pressure measurements in undrained tests indicated that for normally consolidated clays the pore pressure at maximum deviator stress was equal, or nearly so, to the applied deviator stress—but for other soils it was not. This observation has also been reported by other investigators, notably Skempton (4).

The present state of knowledge of the mechanical behavior of cohesion and friction can be summarized briefly as follows: The strength of a clay consists of two components, an effective cohesion, sometimes called the true cohesion, which for a given soil is believed to be a function principally of water content and a frictional component which is the change in frictional resistance due to a change in intergranular stress on a failure plane without change in water content. For normally consolidated clays the total shearing resistance, cohesion plus friction, is believed to be essentially a function of water content. It should be noted that some prominent authors, working with the physico-chemical fundamentals of soil behavior, have expressed doubt about the usefulness and wisdom of separating soil strength into cohesion and friction components (5, p. 20; 6, p. 52).

Basis for this Investigation

The usual use of Mohr's circle in soils is to represent stress conditions at failure, with failure defined as the condition of the soil at the maximum deviator stress or maximum stress ratio. The Mohr failure envelope is the line representing the locus of points showing stress conditions on the failure plane. But since a Mohr's circle represents any two-dimensional stress condition of equilibrium, it can be used at any strain value before failure is reached with the same validity as at the failure conditions conventionally chosen. The envelope formed by points of tangency to the Mohr circles representing intergranular stresses at a point for a given value of strain can be used to find the cohesion and friction at that strain. If the Mohr circles for different intergranular stresses are all found at the same soil structure, the cohesion and angle of internal friction are obtained.

This paper describes a technique for determining Mohr's circles for different intergranular stresses at approximately constant soil structure. Cohesion and friction are computed at various strains and the rate of development of cohesion and friction with strain is thereby determined.

II. DEFINITIONS, EQUIPMENT AND SPECIMEN PREPARATION

Definitions

As has been briefly discussed, there is considerable uncertainty regarding the proper definition and engineering significance of the cohesion and friction

strength components. Perhaps a fresh look at the problem is appropriate. For the purposes of this paper it is assumed that if cohesion and friction can be clearly defined and measured in the laboratory in accordance with these definitions, and these measurements provide useful information, then the usefulness of these measurements is justification enough for the definitions used.

If practicability is to be the justification for the definitions used, then these definitions must deal with at least one of the major reasons why the soil mechanics engineer would like to use the concepts of cohesion and friction. Primarily, he likes the potential simplicity of having the total strength separated into two components—one independent of, and the other dependent upon, intergranular stress. Then, for instance, pore pressure changes would affect only the friction component. The difficulty has been to accomplish this mentally convenient separation in the laboratory.

With the optimistic assumption that this difficulty could be overcome, definitions of cohesion and friction were established at the start of this research. These can be termed the "working definitions" for this research. In this paper the terms "cohesion" and "friction" refer to these definitions. Some comments concerning the degree to which these definitions are "basic" or "fundamental" will be made near the end of this paper, but such considerations will be left primarily to future discussers. The definitions are:

Cohesion (c).—The cohesion of a soil, at any strain, is the shear stress developed on the plane of Mohr envelope tangency at that strain, if the intergranular stress on that plane could be reduced to zero without significant change in soil structure.

Angle of Internal Friction (ϕ).—The angle of internal friction, at any strain, is the angle whose tangent is the ratio of the change in shear stress to the change in normal intergranular stress occurring on the plane of Mohr envelope tangency at that strain, during a stress change occurring without significant change in soil structure.

The intergranular stress is defined in the empirical sense as the total stress less the pore water pressure measured by a piezometer (7). The plane of Mohr envelope tangency is the plane of maximum stress obliquity for the frictional component of strength. For the purpose of specifically locating this plane, it is assumed that cohesion acts isotropically—which may or may not be the case. The interpretation of the word "significant" will be discussed later.

The experimental problem of separating the strength components directly involves a change in intergranular stress. The approach is to change the intergranular stress and interpret the specimen strength changes in terms of the two defined components. Changing the intergranular stress under controlled conditions is conveniently accomplished by controlling the pore water pressure. The concept of using pore water pressure as a test control, rather than just measuring its value in response to other controls, is the heart of the testing technique to be described subsequently.

Equipment

The triaxial equipment used to conduct the research performed herein was purchased from GEONOR A/S, Forskningsveien 1, Oslo-Blindern, Norway, and installed in the South Mechanics Research Laboratory of the University of Florida. It is described in (8). The principal modifications are the use of

Harvard ball-bearing pistons for the triaxial cells (9), and two independent pore pressure devices instead of one. One device is connected to a porous stone under the specimen and the other could be connected to either a needle inserted anywhere in the sample or to the cap on top of the specimen. Provision is made to use only distilled water in the cell and in the pore pressure lines. This water is occasionally de-aired, but stands in contact with air. All tubing is rubber, copper, or plastic.

Throughout most of this work proving rings were used to measure the piston load on the specimen. For triaxial consolidation pressures of 4.15 k/cm^2 and less a ring with an average sensitivity of about 22 g/dial division (0.002 mm) was used. For greater consolidation pressures a ring with an average sensitivity of about 110 g/div. was used. Pore pressure was measured and controlled by means of mercury manometers with an accuracy estimated usually better than $\pm$ 0.02 k/cm^2.

Specimen Preparation

It was originally thought necessary to have available a large number of specimens for this research. The requirements were specimens of clay with as high a degree of saturation as possible and with clay structure duplicated as closely as possible. This includes void ratio, degree of saturation, particle orientation or fabric, mineralogy, and the composition of the double layer and pore water. Such duplication for large numbers of specimens could only be hoped for in remolded specimens.

A "Vac-Aire" extruder, capable of extruding bars of clay of circular or square cross-section with high degree of saturation and structural uniformity was used for specimen preparation (10). With this equipment the action of the extrusion auger in the machine gives the specimen particles a helical orientation—differing from both a random remolding and any orientation due to natural deposition. Any preparation technique is going to give the particles an imposed orientation and as long as this orientation is reproducible a helical one may be as acceptable as any other.

The different clays from which duplicate Vac-Aire extruded specimens were prepared were extruded in a circular bar 3.58 cm in diameter and then immediately cut into 10 cm lengths and waxed. The specimens were stored for a sufficient length of time to complete any thixotropic action, as measured by laboratory vane shear tests. Upon use the wax was carefully removed and the length reduced to 8.00 cm. These were the initial dimensions of the specimen prior to hydrostatic consolidation.

Some undisturbed specimens were also tested. These were trimmed to the same dimensions as the above extruded specimens and generally handled and tested in the same manner.

Each specimen was enclosed by two "Shiek" brand latex protectives. Whatman #54 filter paper was used as protection against soil erosion at the top and bottom and as drainage strips along the side of the specimen. Generally a layer of type M Apiezon grease was applied between the two protective membranes to reduce water and air migration through the membranes. Comparisons of calculated and measured void ratios at the end of the tests show that such migration was not important until the cell pressure reached about 6 k/cm^2, and even then was comparatively minor. However, the duration of the cell pressure application usually did not exceed two days and the same might not be true for longer applications of cell pressure.

III. DEVELOPMENT OF CFS-TEST TECHNIQUE

The term "CFS-test" refers to the laboratory test herein described which attempts to measure the cohesion-friction-strain behavior of a soil. That is, the variation of the defined cohesion and friction strength components over the axial compressive strain range of experimental investigation. The development of this test started with an initial idea which trial and error has continuously modified. This development is still progressing. For the reader's convenience this development is described in three stages: The first was the initial experimental approach involving the use of several specimens for the determination of cohesion and friction, the second which involved the use of only one specimen for a complete CFS determination, and the third stage which involved simplification and a more precise procedure.

Stage 1

Range of Intergranular Stress Chosen.—A method of changing intergranular stress had to be developed which resulted in a minimum of structure change. It was initially decided to take a number of duplicate specimens of a clay, consolidate each to the same hydrostatic pressure, and then perform a series of triaxial compression tests using a different value of intergranular stress for each specimen. The different stress-strain curves obtained could then be compared and the effect of intergranular stress evaluated.

It was necessary to choose which intergranular stress to use; the choices considered were the major ($\bar{\sigma}_1$) or minor ($\bar{\sigma}_3$) principal stresses or the normal stress on the potential failure plane ($\bar{\sigma}_\phi$). It was decided that keeping $\bar{\sigma}_1$ constant was the most practical and would involve the least void ratio change. The intergranular stress was set prior to compression and then held at a constant value of $\bar{\sigma}_1$ by increasing the pore pressure to just match the deviator stress, σ_a (equal to $\sigma_1 - \sigma_3$).

It was realized that two initially identical clay specimens at an identical strain condition, but with different values of $\bar{\sigma}_1$, cannot have exactly the same structure because a void ratio change must occur for the following two reasons:

(a) As the specimen strains the particle alignment (fabric) is continually changing to accommodate the strain. Since the clay is in equilibrium with a given intergranular stress only at a particular fabric and void ratio, any change in fabric will require a void ratio change to maintain the intergranular stress. Then, it follows that any intergranular stress change at a certain fabric (strain) requires a void ratio change.

(b) During the compression the pore water pressure is increased to maintain $\bar{\sigma}_1$ constant. Since σ_3 is held approximately constant then $\bar{\sigma}_3$ must be continually decreasing. This represents a reduction in the total forces of attraction between the clay particles and must be compensated for by a reduction in the total forces of repulsion (5). This is accomplished through an increase in the spacing between the particles, or a void ratio increase.

Thus, some void ratio change and therefore structure change must be expected if the intergranular stress is varied at constant strain or if it is held constant at varying strain.

A compromise had to be reached between minimizing structural changes by minimizing changes in intergranular stress, and increasing accuracy by increasing the change in intergranular stress and therefore the effects of this change that are to be measured. After some study it was decided that a $\bar{\sigma}_1$ range of about 75 to 100 per cent of $\bar{\sigma}_{pct}$ produced strength changes that could be interpreted with sufficient accuracy and yet involved only small void ratio changes. Subsequent measurements have shown that this change is usually less than 1 per cent of the initial void ratio and is thought to be a minor effect in the interpretation of the results. However, this 1 per cent is a swell that may be concentrated in the region of closest contact between adjacent clay particles and could have unexpected importance.

The above describes the interpretation adopted for the expression "without significant change in soil structure" used in the definitions of cohesion and friction. It must be emphasized that the cohesion and friction values determined in this research were computed on the basis of how hydrostatically consolidated specimens behaved under the influence of pore pressure changes that usually varied $\bar{\sigma}_1$ from 75 to 100 per cent of $\bar{\sigma}_{pct}$. Significantly different ranges or magnitudes of $\bar{\sigma}_1$ change may yield different computed results due to the above described complications and are not investigated herein.

Method of $\bar{\sigma}_1$ Control.—An experimental technique was required which would give some assurance that the computed value of $\bar{\sigma}_1$ was representative of the specimen at the time a data observation was made. Since $\bar{\sigma}_1 = \sigma_k + \sigma_a - u$, this involved obtaining a uniform pore pressure within the specimen. This was achieved and measured as follows: The pore pressure at the bottom cap was increased to a value greater than that necessary to match σ_a at that moment and then the pore pressure line was closed. As the specimen subsequently continued to strain and σ_a increase, the pore pressure was also measured at a needle inserted in the upper half of the specimen. When it appeared from the needle and bottom cap pore pressure measurements that the pore pressure was uniform and at the proper value for the $\bar{\sigma}_1$ value chosen, then the data for a stress-strain point were taken. As the specimen continued to strain this procedure was repeated until the maximum desired strain was reached and then a stress-strain curve for that particular value of $\bar{\sigma}_1$ was interpolated through the data points.

The above worked well for the kaolinite used at that time. It usually took less than five minutes for the two pore pressure measurements to agree. The permeability of this clay was about 3×10^{-8} cm/sec. The pore pressure needles were stainless steel, 3.0 cm in length and 0.06 cm in diameter, with approximately 10 small holes along the lower 2 cm of the needle. These were made by GEONOR A/S. These flexible needles were inserted through the double membrane layer and simply sealed with two coats of rubber cement around the insertion point. This type of seal was successful with the 7.15 k/cm^2 maximum cell pressure used.

Example of Stage 1 Results.—An example of the results obtained using the stage 1 technique described is presented in Figs. 1 and 2. Five duplicate specimens of kaolinite were each hydrostatically consolidated to 4.08 k/cm^2 and then each was compressed at a different value of $\bar{\sigma}_1$. The resulting stress-strain curves are presented in Fig. 1(a). It was not possible to hold each point on a curve to exactly the intended $\bar{\sigma}_1$ value, but the variation was only about $\pm$ 5 per cent and a $\bar{\sigma}_1$ value at any particular strain could be interpolated from the nearest measured points on the curve.

Since $\bar{\sigma}_1$ and $\bar{\sigma}_3 = \bar{\sigma}_1 - \sigma_a$ can be interpolated at each value of strain, a Mohr circle can be constructed for the stress conditions within the specimen

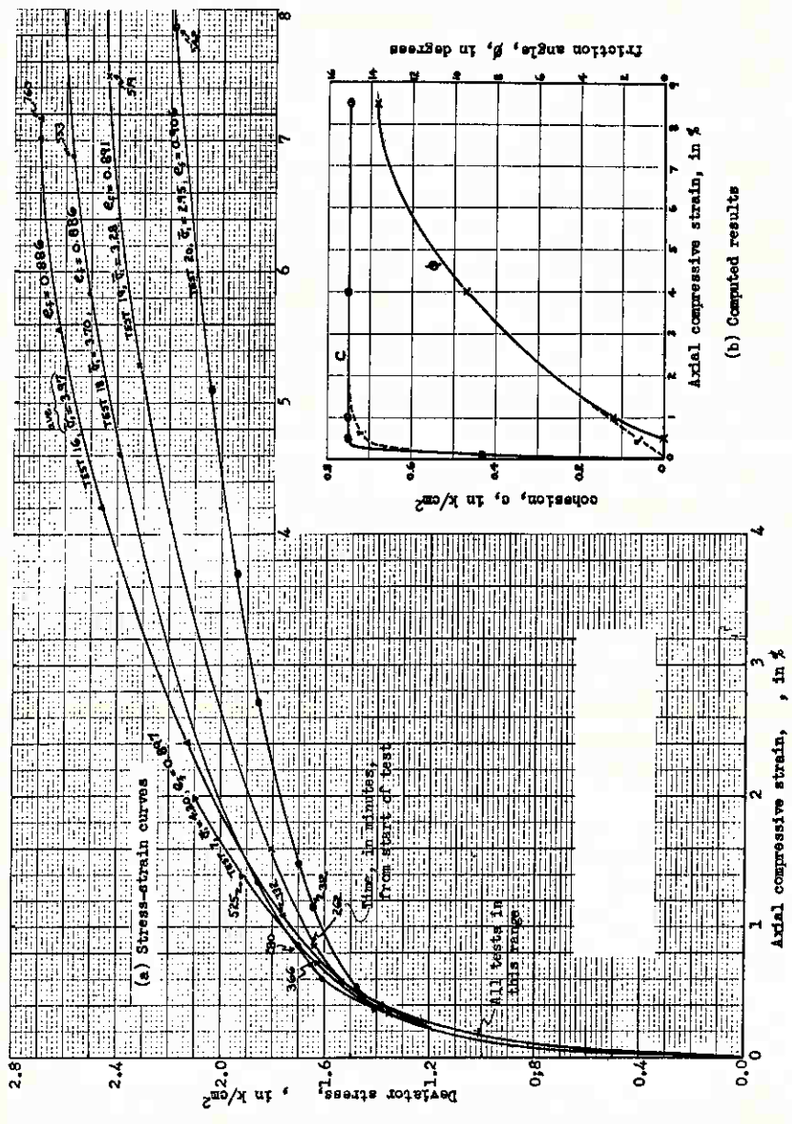

Fig. 1.—Example of Stage-1 CFS-Test Series, DWEPK Samples

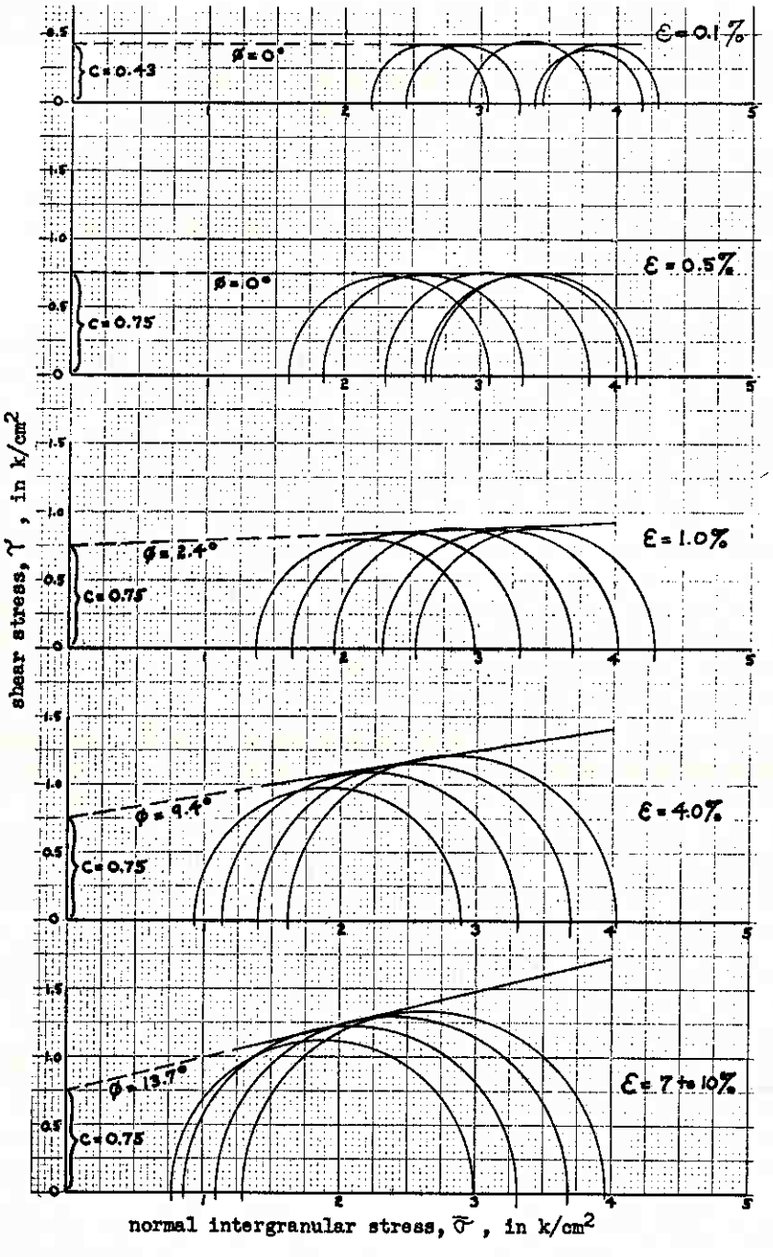

Fig. 2.—Graphs for Stage-1 Extrapolation of Cohesion

at that strain. A separate circle was constructed for each $\bar{\sigma}_1$ curve and the results are presented in Fig. 2 as a series of Mohr circles at each selected strain. The best common tangent to each set of circles was then estimated. The slope of this tangent is the tangent of the angle of internal friction. The $\bar{\sigma}$ = o intercept of the extrapolated tangent is the cohesion component of strength. Thus, the two strength components are separated at different values of strain and a plot can be prepared showing the variation of the components with strain. This is done in Fig. 1(b).

Stage 2

Continued testing showed that important refinements could be made in the CFS-test technique. A number of these were developed in a connected sequence and they are herein presented as the modifications which lead to the stage 2 technique. They are presented in chronological order of development.

Use of Single Specimen.—During the performance of the multiple-specimen CFS-tests of stage 1 it was noticed that deviations from the intended value of $\bar{\sigma}_1$ would result in changes in the deviator stress. It was then thought that it might be possible to vary $\bar{\sigma}_1$ by jumping back and forth to different preselected values, with the specimen continuing to strain, and thereby obtain the same results from one specimen that previously required four. Subsequent experiments showed that this seemed possible—the results from a single specimen would essentially duplicate those from stage 1 multiple-specimen tests, and single specimen test results could be duplicated. This has proved to be a very significant discovery in this research. For the following reasons it has greatly enhanced the practicability of the CFS-test:

(a) Using the same specimen for all four $\bar{\sigma}_1$ stress-strain curves eliminates the inevitable small differences between any set of four duplicate specimens. Because of this a more accurate interpretation of the cohesion and friction strength parameters is possible.
(b) Since duplicates are not required, undisturbed specimens can be tested.
(c) There is a great time saving—one test takes the place of four.

Use of Internal Drain and Elimination of Needle.—It was soon discovered that the major disadvantage of the single-specimen CFS-test was that the pore pressure had to change more rapidly. To use a single specimen the pore water pressure must change to a new equilibrium condition with sufficient speed to obtain an adequate number of points to define all four $\bar{\sigma}_1$ vs. ϵ curves within a day's testing time. This became particularly difficult to accomplish with clays that had a lower permeability than kaolinite.

This difficulty was at least partially overcome by the use of an internal wool drain technique that the writer heard was being used in the soil mechanics laboratory of the firm of Tippetts-Abbett-McCarthy-Stratton, New York, under the direction of Mr. John Lowe, III. Their technique is to prepare compacted triaxial specimens with wool yarn running up the center to speed pore pressure distribution and measurement. Since this research used machine extruded or undisturbed specimens, a technique was devised to insert the wool drains after preparation.

Briefly, the 10 cm specimen is securely placed in a cylindrical miter box with squared ends. The drain pattern to be used is then laid out on each end. The holes for the drains are then punched by a 0.19 cm diameter, stainless steel sewing needle mounted in a small drill press with vertical travel and a

horizontal table. Previously saturated wool yarn is then threaded through the hole of the needle and a double thickness of yarn is pulled through the prepunched hole. The yarn is finally cut off to the exact specimen length when it receives its final trimming to 8.0 cm. The above procedure takes about 15 minutes for a single center drain and about 30 minutes for a 5 drain specimen. During the whole time the specimen sides are protected by the miter box and the final trimming of the ends is the last step before mounting in the triaxial chamber.

Of course, the disturbance due to the punching and the presence of the vertical drainage holes is an undesirable feature. However, the whole operation is neatly done and the volume of 5 holes (the maximum used) is only about 1.2 cm^3, or about 1.5 per cent of the volume of the specimen. It is assumed that the presence of these holes has a negligible effect on the stress-strain curves. It may be that these holes, with their weakening effect, somewhat compensate for the reinforcing effect of the filter paper strips used outside the specimen. In any event the advantages of the internal drains in the performance of the CFS-test seem to far outweigh the possible disadvantages.

A further advantage obtained when internal drains are used is the elimination of the pore pressure needle. Both the control and the measurement of pore pressure can be done at the bottom cap. The direct connection of the drains to the bottom cap insures that the pore pressure is rapidly carried throughout the specimen. This is particularly true in any clay permeable enough to use the needle successfully. For the more impermeable clays, where the pore pressure distribution may not be uniform at a particular time —even with the use of internal drains—the needle will not indicate the lack of uniformity because the very small clay contact area at the needle holes prevents the flow of sufficient water to properly operate the GEONOR pore pressure measuring manometer. Since the needle was used to check the uniformity of pore pressure, and this is better assured by the use of internal drains, the needle is no longer necessary. The elimination of the needle simplified and added to the practicability of the CFS-test.

Use of Point-Line Extrapolation Technique.—The circle-tangent technique to determine ϕ and extrapolate for c was a source of considerable objection in the test analysis. Although it is an easily visualized and direct procedure it is difficult to draw the best tangent to a group of closely spaced circles. The essence of a superior analysis technique is presented on page 166 of reference (11). The accompanying Fig. 3 shows how this technique was adapted for use with the CFS-test. It should be noted that the above method assumes the validity of Equation 1 in Fig. 3. Data presented subsequently will show that this equation of a straight line is experimentally valid over the $\bar{\sigma}_3$ range of 3-4, as shown in Fig. 3(c).

With this improvement the results are plotted as a series of points and one has to fit the best straight line through the points—a much more reproducible procedure.

Example of Stage 2 Results.—Fig. 4 presents the stress-strain curves obtained from a stage 2 test—No. 71. The left-hand side of Table I lists the stress values needed for the preparation of the interpolation-extrapolation graph presented in Fig. 5. The right-hand side of Table I shows the results of using the data from Fig. 5 to compute the c and ϕ components. The variation of c and ϕ with strain is presented in Fig. 6.

Assume the Coulomb-Hvorslev equation governing the failure criteria of homogeneous clay is valid at any axial compressive strain ε .

then:

$$\bar{\tau}_\phi = c_\varepsilon + \bar{\sigma}_\phi \tan \phi_\varepsilon \qquad (1)$$

from Fig. 3 (a)

$$\bar{\tau}_\phi = \frac{\sigma_a}{2} \cos \phi_\varepsilon$$

$$\bar{\sigma}_\phi = \bar{\sigma}_3 + \frac{\sigma_a}{2} - \frac{\sigma_a}{2} \sin \phi_\varepsilon$$

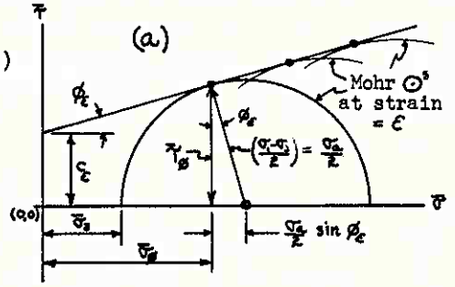

Inserting the expressions for $\bar{\tau}_\phi$ and $\bar{\sigma}_\phi$ into equation (1) and simplifying gives:

$$\frac{\sigma_a}{2} = \left(\frac{\sin \phi_\varepsilon}{1 - \sin \phi_\varepsilon}\right) \bar{\sigma}_3 + c_\varepsilon \left(\frac{\cos \phi_\varepsilon}{1 - \sin \phi_\varepsilon}\right) \qquad (2)$$

which is the expression for a straight line 1-2, with slope m and intercept b, as shown in Fig. 3 (b).

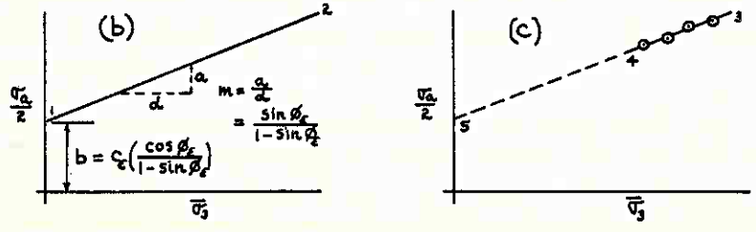

If line 1-2 can be determined experimentally, then at any strain ε :

$$\phi_\varepsilon = \sin^{-1}\left(\frac{a}{d+a}\right) \qquad (3)$$

$$c_\varepsilon = b \left(\frac{1 - \sin \phi_\varepsilon}{\cos \phi_\varepsilon}\right) \qquad (4)$$

The CFS-test is performed to yield values of σ_a and $\bar{\sigma}_3$ at any axial compressive strain. These values are interpolated from the experimental stress-strain curves and plotted as shown in Fig. 3 (c). The best straight line 3-4 is fitted through these points using the rule of least squares if the points are of equal weight, or suitable judgement if they are not. The line is then extended to intercept point 5. The straight line extrapolation of this line is based on the initial assumption of the validity of equation (1). Equations (3) and (4) are then used to compute the values of ϕ_ε and c_ε .

Fig. 3.—Method of Extrapolation for ϕ_ε and C_ε from Results of CFS-Test

Table I.—Computations for Cohesion and Friction
CFS-Test No. 71

Extrapolation of cohesion and friction angle values from C-F test results:

TEST NO. 71

strain	Curve	$\bar{\sigma}_3$	σ_a	$(\bar{\sigma}_3 - \sigma_a)$	$\frac{\sigma_a}{2}$	Computations from extrapolation graph: Friction angle		Cohesion	
0.5 %	⊙	1.90	0.915	0.985	0.457	a	0.457 / .337	b	0.337
	×	1.79	.890	.90	.445	d	0.120 / 1.0	cos φ	0.994
	△	1.72	.875	.845	.437	$\frac{a}{d+a} = \sin\phi$	0.107	1−sin φ / cos φ	0.898
	⊡	1.60	.855	.745	.427	φ	6.1 °	$C = b\left(\frac{1-\sin\phi}{\cos\phi}\right)$	0.303 k/cm²
1.5	⊙	1.92	1.160	.76	.580	a	0.650 / .347	b	0.347
	×	1.82	1.115	.705	.557	d	0.303 / 1.0	cos φ	0.972
	△	1.66	1.060	.600	.530	$\frac{a}{d+a} = \sin\phi$	0.233	$\frac{1-\sin\phi}{\cos\phi}$	0.789
	⊡	1.525	1.005	0.52	.502	φ	13.5 °	$C = b\left(\frac{1-\sin\phi}{\cos\phi}\right)$	0.274 k/cm²
3.0	•	2.055	1.365	.69	.682	a	0.733 / .363	b	0.363
	⊙	1.91	1.295	.615	.647	d	0.370 / 0.8	cos φ	0.949
	×	1.815	1.250	.565	.625	$\frac{a}{d+a} = \sin\phi$	0.316	$\frac{1-\sin\phi}{\cos\phi}$	0.721
						φ	18.4 °	$C = b\left(\frac{1-\sin\phi}{\cos\phi}\right)$	0.262 k/cm²
4.5	◈	2.125	1.470	.655	.735	a	0.699 / .357	b	0.357
	•	2.02	1.41	.61	.705	d	0.342 / 0.6	cos φ	0.932
	⊙	1.93	1.355	.575	.677	$\frac{a}{d+a} = \sin\phi$	0.363	$\frac{1-\sin\phi}{\cos\phi}$	0.683
	×	1.765	1.275	.49	.637	φ	21.3 °	$C = b\left(\frac{1-\sin\phi}{\cos\phi}\right)$	0.244 k/cm²
9.5	+	2.26	1.59	.67	.795	a	0.749 / .366	b	0.366
	◈	2.14	1.52	.62	.76	d	0.383 / 0.6	cos φ	0.921
	•	2.10	1.50	.60	.75	$\frac{a}{d+a} = \sin\phi$	0.390	$\frac{1-\sin\phi}{\cos\phi}$	0.662
	⊙	1.95	1.415	.535	.707	φ	23.0 °	$C = b\left(\frac{1-\sin\phi}{\cos\phi}\right)$	0.242 k/cm²

Since these will be of interest in subsequent discussion a number of representative figures similar to Fig. 5, but obtained from other stage 2 tests on different soils, have been included herein. These are designated Figs. 7, 8, 9, and 10.

Stage 3

The stage 2 technique appeared to be reasonably satisfactory until it proved difficult for the average student to grasp. Much specialized technique and experience was required to jump from one curve to another. A method was sought that would systematize the procedure and would permit anyone familiar with triaxial testing to obtain reproducible results from a set of instructions and a simple demonstration. This search took several months and resulted in a further improved technique which is the one now used (Feb. 1960) and is referred to as the stage 3 technique.

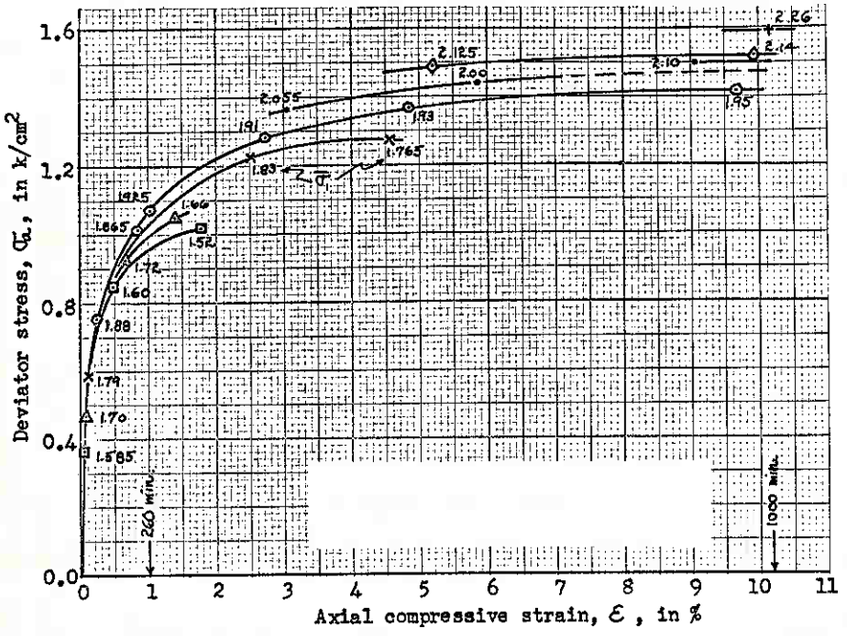

Fig. 4.—Stress-Strain Curves CFS-Test No. 71 Sample Q-BBC 713

Constant Rate-of-Strain, New Load Cell.—The triaxial equipment used is designed such that the loading table moves up at a constant rate against a proving ring. The rate-of-strain in the specimen varies with how the table movement is shared between the ring and the specimen. For a test carried to 10 per cent strain the compression is about 8 mm. If the proving ring is used to capacity its compression is about 2.7 mm. In the early part of the strain almost all of the table movement is used to compress the ring, while in the high-strain part of the test almost all is going into specimen compression. In addition to the above, which would be encountered in any type of test, shifting from one $\bar{\sigma}_1$ curve to another is required. Each shift requires that the proving ring compress or extend. Thus, the stage 2 technique involved a rather complicated rate-of-strain sequence that was far from a constant rate test.

In order to eliminate possible complications due to changes in the rate-of-strain, and to improve the simplicity with which the test is performed, it was decided to develop a more constant rate-of-strain test. To accomplish this a less compressible load measuring device was developed.

The proving ring is now replaced with an aluminum tube, 6 inches long, 3/8 inches O.D., and 0.030 inches wall thickness. The center two inches of this tube is machined to a reduced wall thickness. In the case of the load cell used to replace the 30 k proving ring this reduced wall thickness is about 0.003 inches. Four SR-4 strain gages, type C-7, are mounted on this portion of the tube. Two opposite longitudinal gages measure compression and compensate for bending, and two opposite circumferential gages are for temperature compensation and additional sensitivity due to the Poisson effect.

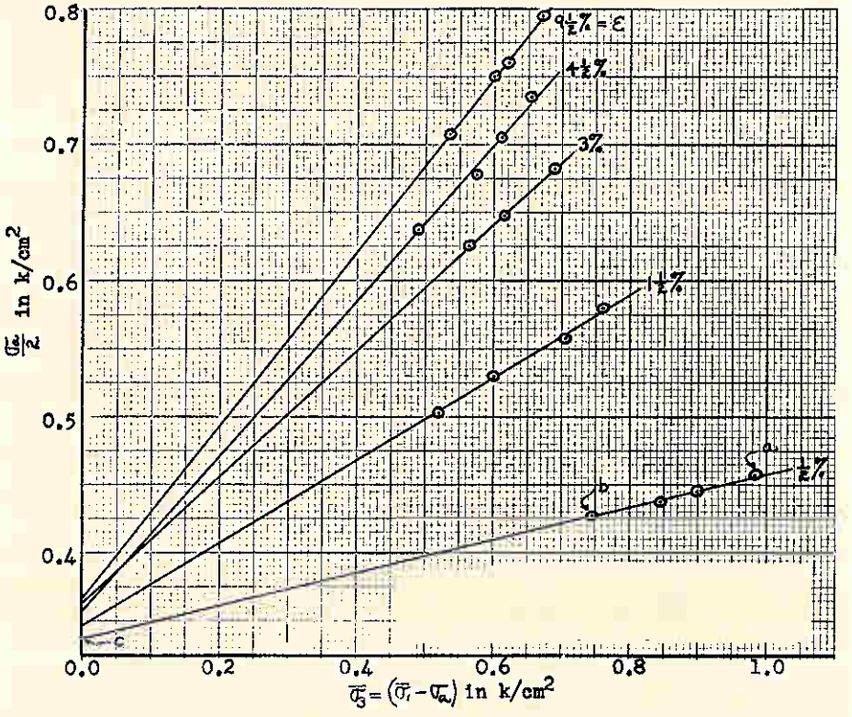

Fig. 5.--Graph for Extrapolation of Cohesion CFS-Test No. 71, Sample Q-BBC 713

A load cell thus constructed gives a convenient linear calibration curve, which the replaced proving rings did not have. The sensitivity is better than 100 grams load per 100 microinches/inch strain, or one full division on the SR-4 strain indicator. By setting the gage factor scale on the indicator to the proper value the calibration can be made exactly 100 grams/full division. This conveniently eliminates the need for a calibration curve and provides more than adequate sensitivity. The three cells built to date (Feb. 1960) have proved durable, easy to build and use, give stable strain indicator readings, and yield reproducible calibration curves. Over the same load ranges as the proving rings which they replaced these cells have only about 1/15 the

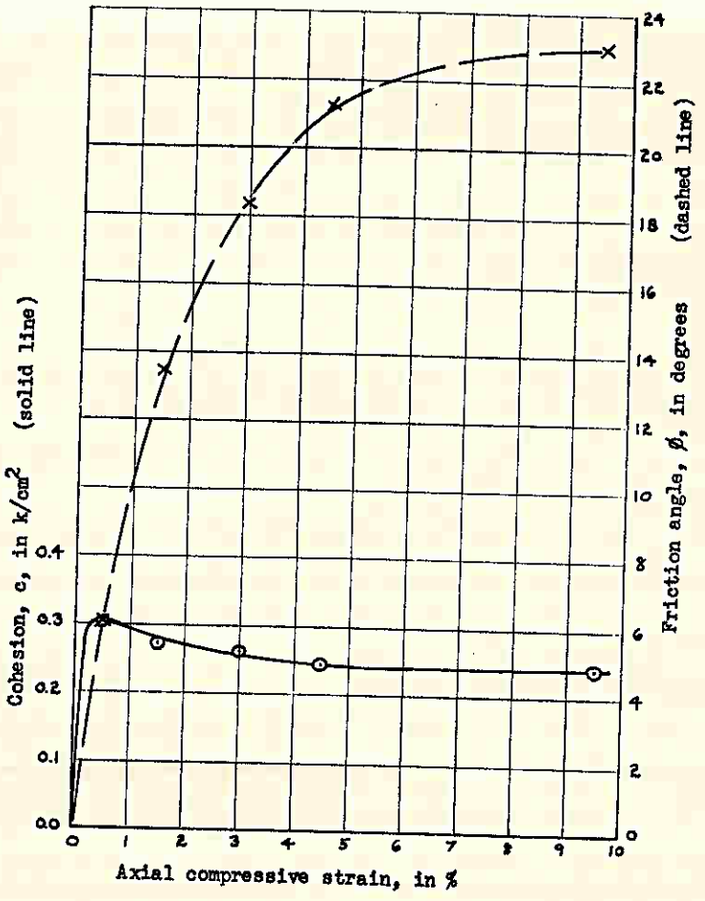

Fig. 6.—Computed Results, CFS-Test No. 71 Sample Q-BBC 713

compression of the rings. A loading system using these cells is more rigid and the CFS-tests are carried out at close to a constant rate-of-strain.

The constant compression rate used is 0.005 mm/min, or somewhat less than 1/2 per cent axial compressive strain per hour for the 80 mm initial height of the specimens used. This rate has been found slow enough to permit obtaining enough data points with adequate pore pressure uniformity and yet reach 3 to 4 per cent strain in an 8 hour testing day. The test can be left to run overnight and additional data obtained the next morning at about 9 to 10 per cent strain.

New $\bar{\sigma}_1$ Curve-Hopping Technique.—Inspection of the many graphs obtained similar to those presented in Figs. 5 and 7 to 10 indicated that the points almost always fell close to a straight line over the experimental $\bar{\sigma}_1$ range used. This suggested the possibility that only the end points, such as "a" and "b"

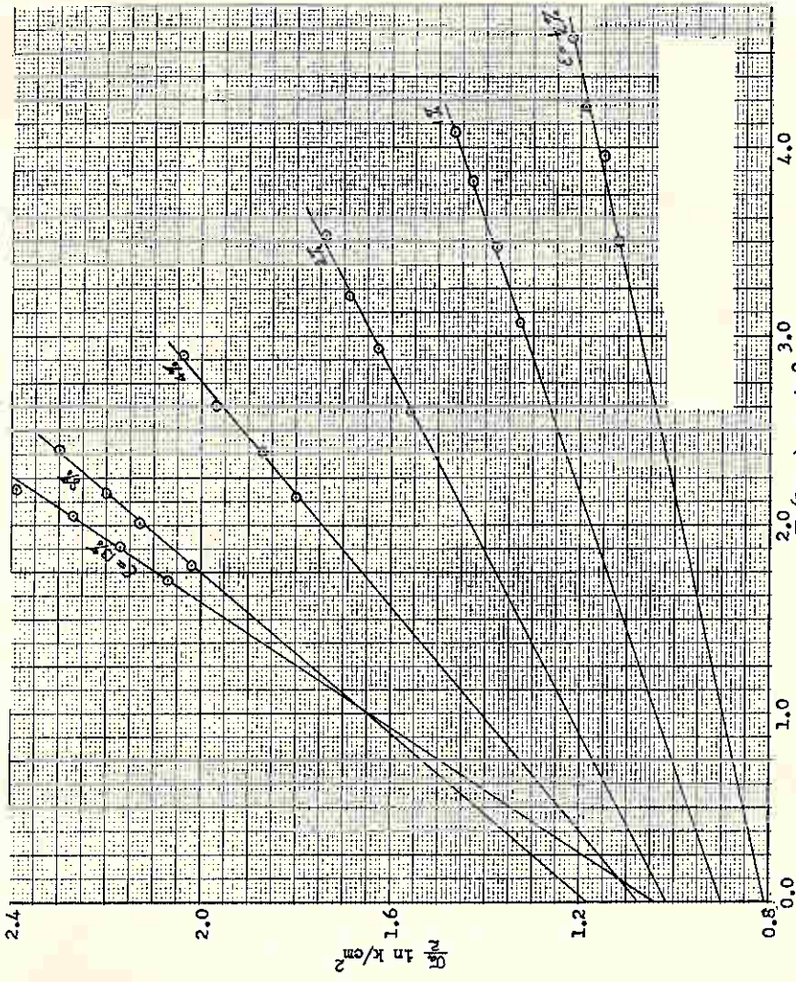

Fig. 7.—Graph for Extrapolation of Cohesion CFS-Test No. 53, Sample DWEPK 614

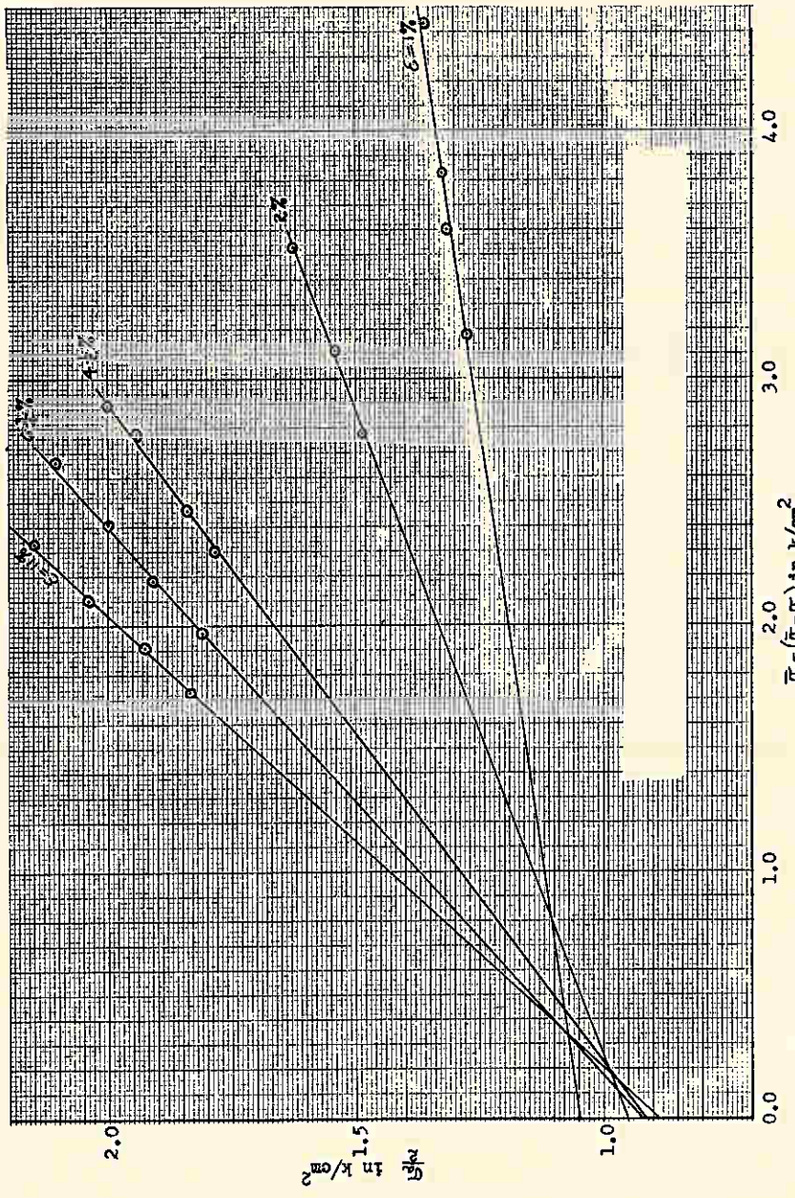

Fig. 8.—Graph for Extrapolation of Cohesion CFS-Test No. 73, Sample BBC 518

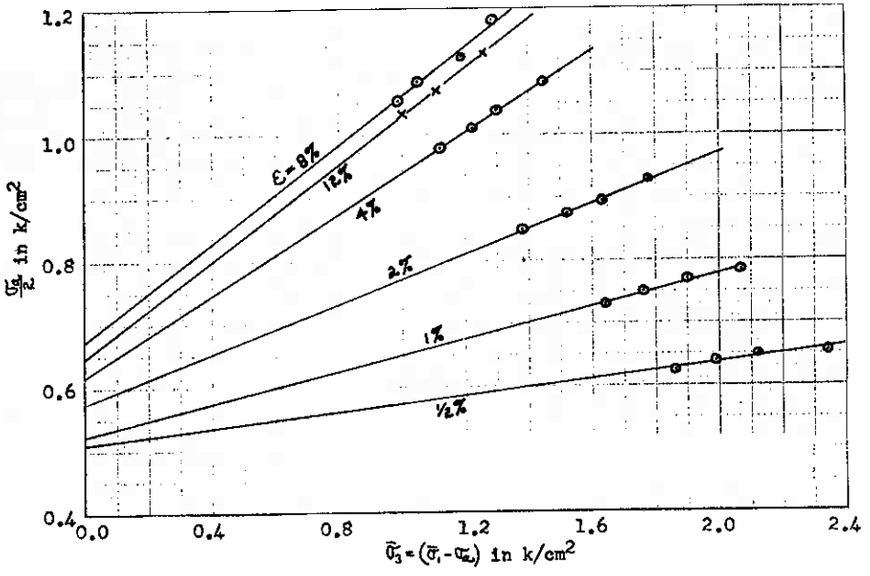

Fig. 9.—Graph for Extrapolation of Cohesion CFS-Test No. 49, Sample N-EPK 412

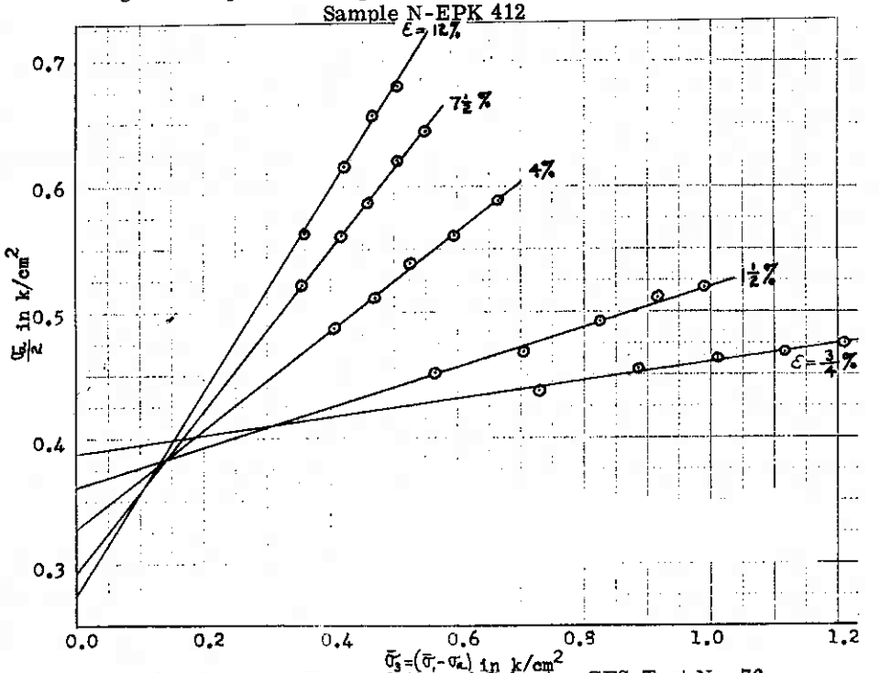

Fig. 10.—Graph for Extrapolation of Cohesion CFS-Test No. 76, Sample JSC 758

in Fig. 5, need be determined and the line a-c then be constructed directly through the two points. This would further simplify the CFS-test and make the analysis more reproducible by eliminating the need to fit the best straight line through a series of points. This line is now drawn directly through the two points or, more recently, computed mathematically and thereby eliminates all graphical errors in this part of the analysis.

Since only the two end points, instead of the previous four, are to be used to determine ϕ and extrapolate for c, these points have to be accurately determined. It was therefore decided to obtain two successive points on each outside $\bar{\sigma}_1$ curve before hopping to the other curve. Since only two $\bar{\sigma}_1$ curves are used this permits more time for $\bar{\sigma}_1$, or pore pressure equilibrium. This is particularly true for the second point. This procedure has lead to a more accurate positioning of each $\bar{\sigma}_1$ curve and thereby not only simplified the cohesion and friction computations but also increased accuracy.

Final Technique for $\bar{\sigma}_1$ Curve-Hopping.—The following account is presented to give the step by step procedure in the most recent technique developed. Reference will be made to Fig. 11 which shows a schematic diagram of the triaxial set-up during the compression part of the CFS-test, and to Fig. 12 which shows a portion of the stress-strain curves obtained. The procedure is as follows:

(a) Points 1 and 2 are obtained on the high $\bar{\sigma}_1$ curve.
(b) The pore pressure at the bottom of the specimen is then increased by the difference between the $\bar{\sigma}_1$ values selected for each curve. This difference is $\Delta\bar{\sigma}_1$. The increase is accomplished by using the screw control I to force water into mercury manometer a and increase the Δa value. The total pore pressure at the bottom of the specimen is the value in hydraulic load cell A plus Δa.
(c) This pore pressure change is carried throughout the specimen by means of the system of external filter paper and internal wool drains.
(d) As the pore pressure is increasing $\bar{\sigma}_1$ decreases and this decrease is followed by the SR-4 load cell. During this decrease in $\bar{\sigma}_1$ the screw control I is used to periodically reduce Δa to keep the value of $\bar{\sigma}_1$ constant at the low value at the bottom of the specimen.
(e) After some time, but usually within 15 minutes, σ_a levels off and starts to increase as if it was following the low $\bar{\sigma}_1$ curve. It is now assumed that the specimen has reached an adequate stage of pore pressure equilibrium and the data for point 3 are taken.
(f) Additional time is allowed, usually a minimum of 15 minutes, while the specimen strain is continued at the same controlled value of $\bar{\sigma}_1$. Then the data for point 4 are taken. It is assumed that this point is more accurately positioned on the selected curve than point 3 because more time has been allowed for $\bar{\sigma}_1$ equilibrium.
(g) If points 3 and 4 appear to be on the same $\bar{\sigma}_1$ curve then the pore pressure adjustments are made to reach point 5. If they do not agree an additional point is taken on the lower $\bar{\sigma}_1$ curve and the first point 3 is disregarded as premature.
(h) The pore pressure is then decreased by the amount $\Delta\bar{\sigma}_1$. This is accomplished by reducing Δa with screw control I. This decrease causes a small volume reduction in the specimen. Because of the rigid load cell the volume reduction results in a drop of load carried by the cell. This is, however, quickly recovered without further change in pore

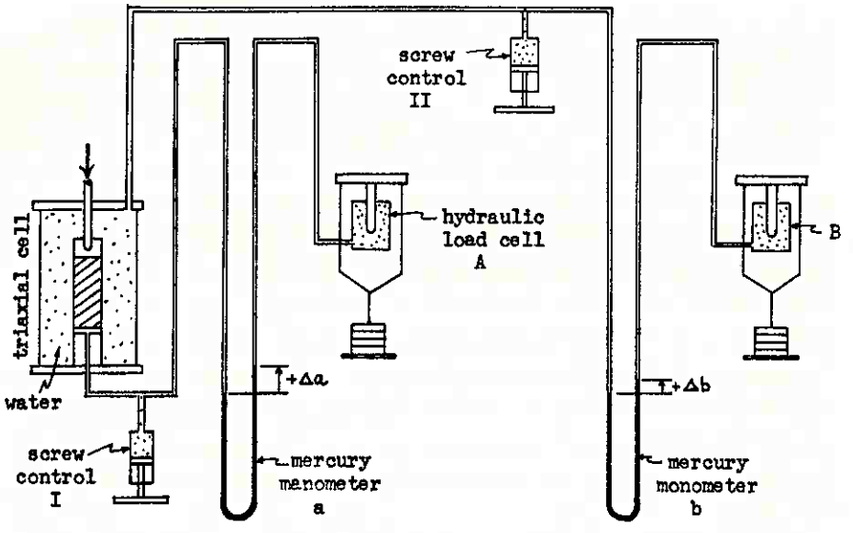

Fig. 11.—Schematic Diagram of Triaxial Apparatus During CFS-Test

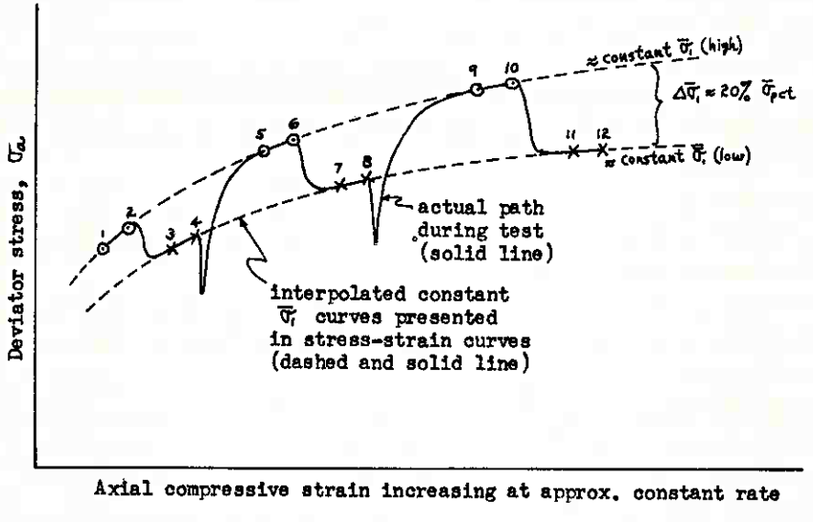

Fig. 12.—Some Details of Stage-3 $\bar{\sigma}_1$ Curve Hopping Technique

pressure and soon the σ_a value is greater than its value at point 4.

(i) As the σ_a value continues to increase the pore pressure at the bottom cap is periodically adjusted to keep the high $\bar{\sigma}_1$ value constant at the bottom cap.

(j) After some time, usually a minimum of 1/2 hour, the rate of increase of σ_a decreases and it appears as if the specimen is following the high $\bar{\sigma}_1$ curve. It is now assumed that the specimen has reached an adequate stage of pore pressure equilibrium and the data for point 5 are taken.

(k) Additional time is allowed, usually a minimum of 15 minutes, while the strain continues at the same value of $\bar{\sigma}_1$. Then the data for point 6 are taken. It is again assumed that this point is more accurately positioned than the preceding point 5 because more time has been allowed for $\bar{\sigma}_1$ equilibrium.

(l) Points 5 and 6 are compared and if it seems that point 5 was premature an additional point at the high $\bar{\sigma}_1$ value is obtained and the first point 5 is disregarded.

(m) The pore pressure at the bottom of the specimen is then increased by $\Delta\bar{\sigma}_1$ and points 7, 8, 9, etc. are obtained by the same procedures.

The volume change of the specimen throughout the test is measured by continually observing the changing magnitude of Δb at mercury manometer b. Any change in specimen volume causes a change in Δb. The cell pressure is the pressure in load cell b plus Δb. Screw control II is used to keep the magnitude of Δb small and thus the cell pressure is almost constant. The triaxial unit is in an air-conditioned room with the temperature essentially constant. Appropriate corrections are made for oil seepage past the piston and for piston travel into the cell. The measured volume changes are used to determine void ratio changes during the test and also to correct the specimen compression readings for that portion due to these volume changes. The latter is usually a minor correction.

Examples of Stage 3 Results.—Fig. 13(a) presents the stress-strain curves from the first complete stage 3 test performed. This test was performed by John R. Hall, Jr., graduate assistant in the University of Florida Soil Mechanics Research Laboratory. Fig. 14 and Table II present the cohesion-friction-strain analysis for this test, with the results plotted in Fig. 13(b). Other examples are included in the following section of this paper.

An Ottawa sand was tested to evaluate the accuracy of the cohesion measurement using the stage 3 CFS-test technique. This sand had all grains between the Nos. 30 and 40 U. S. Std. sieves. Of course the cohesion of this sand is zero. The cohesion values obtained from a stage 3 CFS-test gave some idea of the cohesion errors associated with this test. The results of this test are presented in Fig. 15.

It may be seen from the above figure that the computed cohesion varies from 0.008 to 0.059 k/cm^2. This error is most likely due to the double membrane used. There may be some contribution due to capillarity from incomplete saturation. The usual value for the cohesion of a clay preconsolidated to the same pressure is about 0.65 k/cm^2. Thus, a clay with the same friction angle at a given strain as the Ottawa sand would have a maximum CFS-test cohesion error of about 0.06 k/cm^2. However, in the early strain part of the test any clay, even a very sandy one, would have a friction angle less than half that of this sand. The membranes would then be less than half as effective in introducing error.

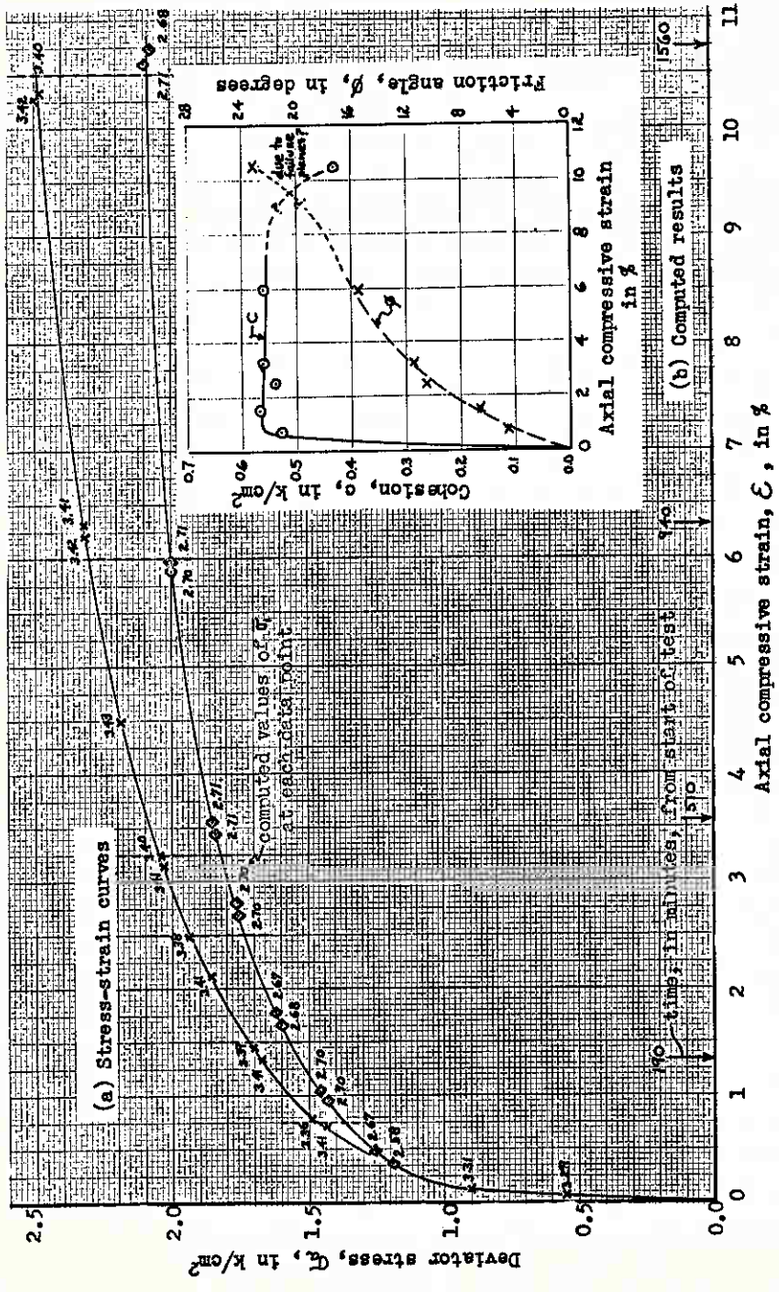

Fig. 13.—CFS-Test No. H13, Sample DWEPK 799

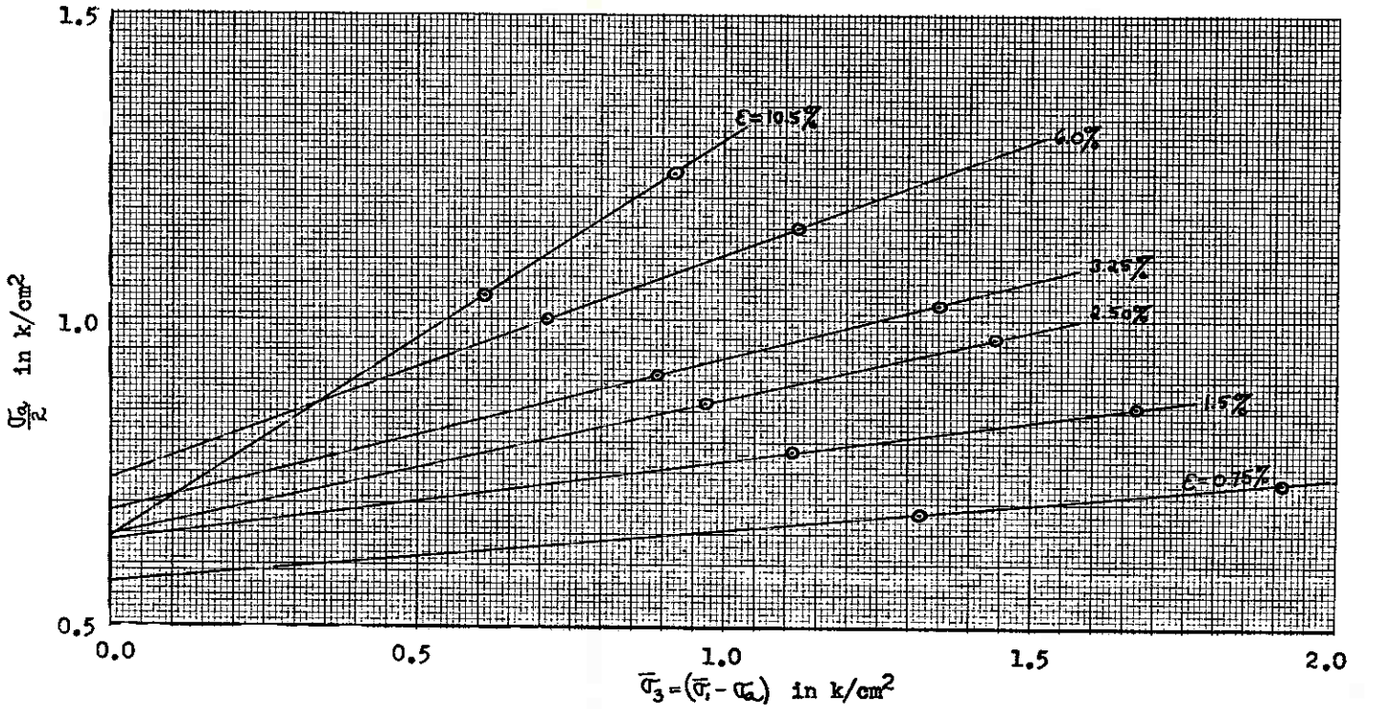

Fig. 14.—Graph for Extrapolation of Cohesion CFS-Test No. H13, Sample DWEPK 799

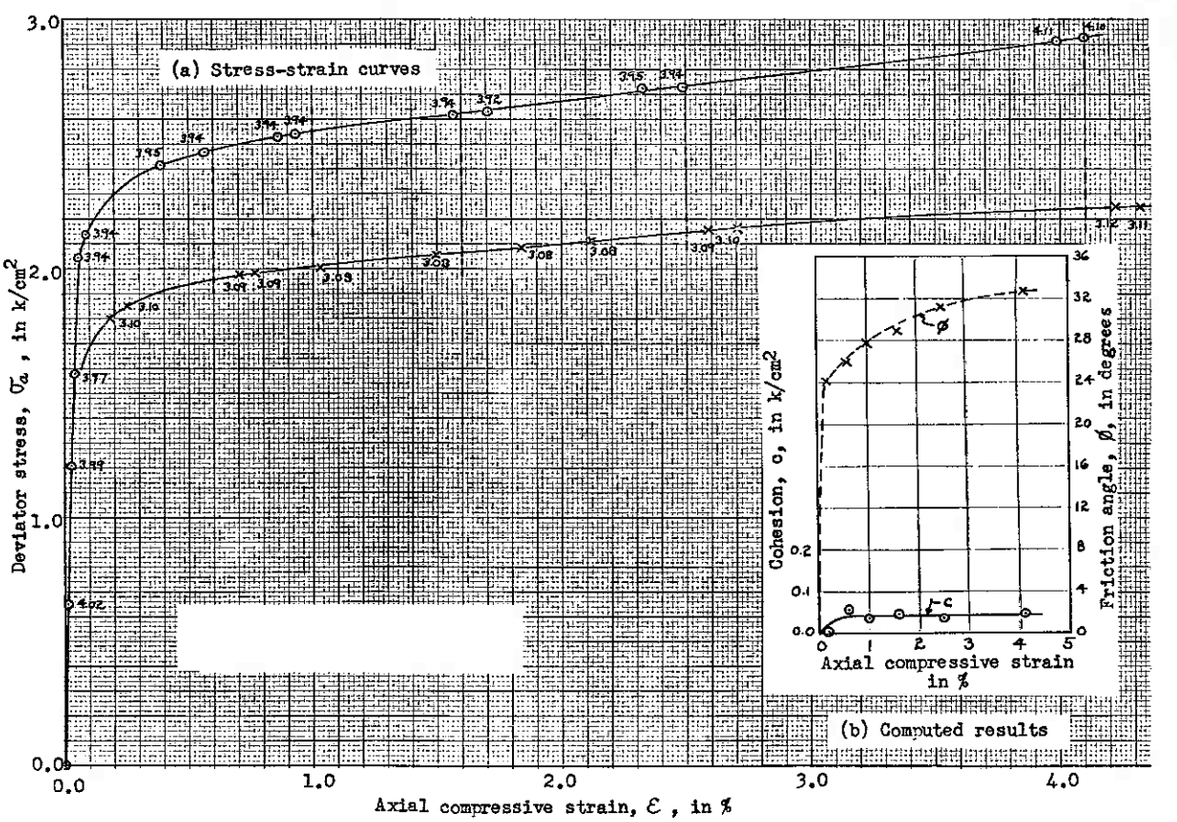

Fig. 15.—CFS-Test No. 93, Ottawa Sand

Table II.—Computations for Cohesion and Friction
CFS-Test No. H-13

Extrapolation of cohesion and friction angle values from CF-Test results:

TEST NO. H-13

strain	Data for extrapolation graph: curve	$\bar{\sigma}_1$	σ_a	$(\bar{\sigma}_1 - \sigma_a)$	$\left(\frac{\sigma_a}{2}\right)$	Computations from extrapolation graph: Friction angle		Cohesion	
0.75 %						a	$\frac{0.743}{0.570}$	b	0.570
	×	3.38	1.47	1.91	0.735	d	$\frac{0.173}{2.0}$	$\cos\phi$	0.997
	◇	2.69	1.37	1.32	0.685	$\frac{a}{d+a} = \sin\phi$	0.080	$\frac{1-\sin\phi}{\cos\phi}$	0.923
						ϕ	4.6°	$C = b\left(\frac{1-\sin\phi}{\cos\phi}\right)$	0.53 k/cm²
1.50						a	$\frac{0.835}{0.640}$	b	0.640
	×	3.39	1.72	1.67	0.86	d	$\frac{0.195}{1.5}$	$\cos\phi$	0.993
	◇	2.68	1.57	1.11	0.785	$\frac{a}{d+a} = \sin\phi$	0.115	$\frac{1-\sin\phi}{\cos\phi}$	0.891
						ϕ	6.6°	$C = b\left(\frac{1-\sin\phi}{\cos\phi}\right)$	0.57 k/cm²
2.50						a	$\frac{0.983}{0.647}$	b	0.647
	×	3.38	1.94	1.44	0.97	d	$\frac{0.336}{1.5}$	$\cos\phi$	0.983
	◇	2.70	1.73	0.97	0.865	$\frac{a}{d+a} = \sin\phi$	0.183	$\frac{1-\sin\phi}{\cos\phi}$	0.831
						ϕ	10.5°	$C = b\left(\frac{1-\sin\phi}{\cos\phi}\right)$	0.54 k/cm²
3.25						a	$\frac{1.064}{0.688}$	b	0.688
	×	3.40	2.05	1.35	1.025	d	$\frac{0.376}{1.5}$	$\cos\phi$	0.980
	◇	2.71	1.82	0.89	0.91	$\frac{a}{d+a} = \sin\phi$	0.200	$\frac{1-\sin\phi}{\cos\phi}$	0.816
						ϕ	11.5°	$C = b\left(\frac{1-\sin\phi}{\cos\phi}\right)$	0.56 k/cm²
6.0						a	$\frac{0.740}{0.552}$	b	0.740
	×	3.42	2.30	1.12	1.15	d	$\frac{0.552}{1.5}$	$\cos\phi$	0.963
	◇	2.71	2.00	0.71	1.00	$\frac{a}{d+a} = \sin\phi$	0.269	$\frac{1-\sin\phi}{\cos\phi}$	0.759
						ϕ	15.6°	$C = b\left(\frac{1-\sin\phi}{\cos\phi}\right)$	0.56 k/cm²
10.5						a	$\frac{1.294}{0.645}$	b	0.645
	×	3.40	2.48	0.92	1.24	d	$\frac{0.649}{1.0}$	$\cos\phi$	0.920
	◇	2.69	2.08	0.61	1.04	$\frac{a}{d+a} = \sin\phi$	0.393	$\frac{1-\sin\phi}{\cos\phi}$	0.660
						ϕ	23.1°	$C = b\left(\frac{1-\sin\phi}{\cos\phi}\right)$	0.43 k/cm²

The writers believe that if sufficient data points are obtained to interpolate the $\bar{\sigma}_1$ curves, and sufficient time is allowed for $\bar{\sigma}_1$ equilibrium as described in the procedure, then the error in determining peak cohesion by the CFS-test is less than 0.05 in 0.65 k/cm^2, or less than 10 per cent.

It is believed that the CFS-test is now at the stage where it is a practical, reproducible, and accurate test for the measurement of the strain variation of cohesion and friction as defined herein. This test requires only a single specimen and can be performed on almost any saturated, remolded or

undisturbed soil. Possible exceptions are highly impermeable and highly swelling clays. These remain to be investigated.

IV. ADDITIONAL EXPERIMENTAL RESULTS

As has been explained, the development of the CFS-test has been a process of successive improvements. Therefore all the data obtained have not been of uniform quality and, for instance, an early stage 2 test repeated with stage 3 technique would probably yield somewhat different results. However, these differences are believed to be primarily due to refinements in detail and consistency, with the basic cohesion-friction-strain behavior remaining the same. In spite of this non-uniformity in the quality of the experimental results, they are presented for completeness.

The results are presented in a number of graphical forms. The main body of experimental results are from the stage 2 testing of extruded specimens. To this has been added some recent stage 3 tests on undisturbed specimens. The common reference by which each test can be identified is by test number. Preceding the graphical presentation is Table III, which presents, in order of test number, information about the type of soil used and the testing conditions. In all cases each specimen was hydrostatically consolidated for a period of about 20 hours, by which time it was in the secondary compression range, and then tested in compression using the controlled $\bar{\sigma}_1$ conditions of the CFS-test technique. The compression test usually took from 10 to 15 hours.

Soils Used

Extruded Specimens

As has been mentioned, all remolded specimens were prepared by extrusion from the Vac-Aire machine. The number prepared at one extrusion session varied from about 15 to 55. Although the machine built-in an unnatural clay structure, the specimens were highly reproducible and it is because of this overwhelming advantage that this preparation method was used. A number of different clays were used to provide some variety in mineralogy, and two of the clays were prepared with chemical additives in an attempt to obtain variations in structure for constant mineralogy. Some information on the Atterberg limits, specific gravity, extruded void ratios and degree of saturation for the different clays is presented as part of Table III.

Kaolinite.—The first specimens tested in this research were kaolinite from the Edgar Plastic Kaolin Co., in Edgar, Fla. As described in reference (12), this is a particularly pure commercial kaolinite. The kaolinite was received in dry, powdered form. It was then mixed with distilled water in its "as received" form. This group of specimens is designated as DWEPK. In the laboratory vane shear test this soil shows a sensitivity of about 2.2 with an extruded water content of 43 per cent, and about 3.5 when the extruded water content is about 34 per cent.

Another group of specimens was prepared using the same "as received" kaolinite, but the powdered kaolinite was mixed with a 1/30 molar solution of di-sodium phosphate ($Na_2HPO_4 \cdot 7H_2O$). This additive resulted in the reduction of the PI of the clay from 21 to 8 per cent, a reduction in strength, sensitivity and permeability at a constant void ratio, in the reduction of the

Table III.—Chronological Test Summary

Test No.	Sample Type	Sample No.	Date Made	Date Tested	(59-60) Limits LL	(59-60) Limits PI	G	As Extruded e_o	As Extruded S_o	$\bar{\sigma}_{pct}$	Test Time (min)	Max. Test Δe
7	DWEPK	465	16 Jan	24 Feb	52	21	2.61	1.034	99.3	4.21	652	
16	DWEPK	490	16 Jan	12 Mar	52	21	2.61	1.055	99.3	4.08	760	
18	DWEPK	491	16 Jan	16 Mar	52	21	2.61	1.049	99.4	4.08	595	
19	DWEPK	492	16 Jan	18 Mar	52	21	2.61	1.050	99.2	4.08	681	
20	DWEPK	493	16 Jan	20 Mar	52	21	2.61	1.047	99.6	4.08	605	
40	DWEPK	610	15 Apr	3 Jun	52	21	2.61	1.022	99.5	1.15	988	
41	DWEPK	611	15 Apr	5 Jun	52	21	2.61	1.018	99.5	2.12	905	
42	DWEPK	612	15 Apr	8 Jun	52	21	2.61	1.022	99.5	3.62	921	
43	DWEPK	613	15 Apr	10 Jun	52	21	2.61	1.019	99.5	7.02	723	
48	N-EPK	411	9 Jan	26 Jun	36	7	2.61	0.857	99.8	2.15	644	No
49	N-EPK	412	9 Jan	29 Jun	36	7	2.61	0.858	99.4	3.64	642	Data
50	N-EPK	413	9 Jan	1 Jul	36	7	2.61	0.849	99.6	1.17	625	
51	N-EPK	414	9 Jan	3 Jul	36	7	2.61	0.854	99.7	7.05	840	
52	N-EPK	415	9 Jan	8 Jul	36	7	2.61	0.850	99.7	6.10	615	
53	DWEPK	614	15 Apr	10 Jul	52	21	2.61	1.030	99.2	7.10	850	
56	N-EPK	416	9 Jan	19 Jul	36	7	2.61	0.856	99.9	6.10	775	
60	BBC	513	11 Mar	28 Jul	38	19	2.81	0.756	98.0	3.65	822	
61	BBC	514	11 Mar	30 Jul	38	19	2.81	0.754	97.4	2.16	816	
62	BBC	515	11 Mar	1 Aug	38	19	2.81	0.754	98.0	1.17	705	
63	BBC	516	11 Mar	4 Aug	38	19	2.81	0.750	98.3	7.15	815	
69	Q-BBC	711	13 May	20 Aug		11	2.81	0.615	99.3	5.65	759	+.002
70	Q-BBC	712	13 May	23 Aug		11	2.81	0.619	99.5	3.40	821	+.002
71	Q-BBC	713	13 May	25 Aug		11	2.81	0.615	99.7	1.91	998	+.004
72	Q-BBC	714	13 May	27 Aug		11	2.81	0.620	99.2	8.15	958	-.002
73	BBC	518	11 Mar	29 Aug	38	19	2.81	0.751	99.2	7.15	861	-.003
74	JSC	756	15 May	1 Sep	30	14	2.72	0.673	100.4	7.15	829	-.003
75	JSC	757	15 May	3 Sep	30	14	2.72	0.673	100.2	3.65	750	-.004
76	JSC	758	15 May	6 Sep	30	14	2.72	0.679	100.8	2.16	867	-.004
77	JSC	759	15 May	8 Sep	30	14	2.72	0.674	99.2	1.17	840	-.005
H13	DWEPK	799	23 Oct	11 Dec	52	21	2.61	1.064	99.8	3.65	1560	+.003
88	U-LC	3R/7		8 Jan	80	56	2.84	2.084	99.0	2.00	795	+.011
89	U-M	I-I		24 Jan	69	45	2.73	0.943	98.1	5.15	766	+.006
91	U-BBC	4		28 Jan	35	15	2.81	0.965	99.7	4.00	906	+.005
92	U-EPK			30 Jan				0.563	76.8	4.00	743	+.006
93	Ott. sand			3 Feb		0	2.65	0.519	100	4.06	741	

equilibrium void ratio at a given consolidation pressure, and in the reduction of the compression index and rate of secondary consolidation for a given consolidation pressure increment (13). This evidence is taken to support the conclusion that di-sodium phosphate kaolinite, herein given the designation N-EPK, has a more dispersed structure than the DWEPK.

Boston Blue Clay.—A series of duplicate specimens of Boston Blue Clay was extruded for this research. The clay was obtained from a pit in Cambridge, Mass. It is herein designated as BBC. The clay was machine remolded at its natural water content and then allowed to dry partially. After it had gained sufficient strength to permit Vac-Aire extrusion this was done with no addition of water. Thus, the clay was extruded with only the natural water in the specimen. Grain size analysis showed that 98 and 43 per cent of this clay, by weight, was finer than the No. 200 sieve (0.074 mm) and 2 microns, respectively.

Another group of specimens was prepared from the BBC, but one part of sodium tetraphosphate ($Na_6P_4O_{13}$), commercially known as "Quadrofos," was added to about 475 parts of clay (dry weight) before the extrusion process. This reduced the PI of the clay from 19 to 11 per cent. For comparison it may be of interest to note that the PI of the kaolinite was reduced to about 4 per cent when the "as received" powder was mixed with a 1/25 molar solution of Quadrofos. Although detailed comparative tests were not performed on the Boston Blue Clay specimens, as they were for the kaolinite, it is assumed that the similar action of the polyphosphate additive also resulted in a more dispersed structure for the Quadrofos Boston Blue Clay when compared with the "natural" BBC. This clay is herein given the symbol Q-BBC.

Jacksonville Sandy Clay.—It was thought to be of interest to test a clay that had a significant percentage of coarser grains. To obtain such a clay a large number of split spoon specimens, taken from the same layer of soil in Florida and stored in tightly sealed jars, were mixed together. The resulting specimens are called "Jacksonville Sandy Clay" and are designated JSC. These were extruded with only the natural water in the clay. A wet sieve analysis indicated that 38 per cent of the clay, by weight, was coarser than the No. 200 sieve (0.074 mm). The clay has a definite gritty feel when worked between the fingers.

Undisturbed Specimens

The CFS-testing of saturated, undisturbed specimens presents no special difficulty. The specimen must be firm enough to trim and handle. Within this limitation, the present experience indicates that any undisturbed cohesive soil can be satisfactorily tested using the stage 3 CFS-test technique. A possible limitation which has not yet been investigated is the testing of highly impermeable, swelling clays. In order to clearly demonstrate that the CFS-testing of undisturbed specimens is a practical matter, a number of undisturbed specimens were tested by the phase 3 technique and the results are included in this paper.

Test No. 91 was performed on an undisturbed specimen of Boston Blue Clay. The clay was obtained from Hewes Clay Pit in W. Cambridge, Mass. The use of this clay permits an opportunity to compare the results of CFS-tests on both undisturbed and extruded specimens of Boston Blue Clay. However, these clays are not completely comparable. Minus No. 200 sieve and 2 micron values of 100 and 46 per cent compare favorably but the limits are somewhat different.

Test No. 89 was performed on a specimen obtained from a 5 inch diameter undisturbed specimen of a stiff, mottled, blue and orange clay with iron oxide discolorations indicating previous irregular crack planes. This clay is somewhat brittle, with a tendency to break apart along these crack planes. Such cracking took place due to the wedging action associated with the insertion of the necessary internal drains (three used) but these cracks appeared to heal during consolidation and the failure planes did not follow them. This clay was obtained from the U. S. Army, Corps of Engineers laboratory at Marietta, Ga., and is designated U-M1.

In addition, single tests were performed on two clays that are somewhat extreme in character. The first test, No. 88, was on a specimen of soft, highly plastic, impermeable clay from New Orleans, La. The clay was almost too soft to trim and handle. The second test, No. 92, was on an undisturbed specimen of the "clay" mined at the Edgar Plastic Kaolin Co. About

73 per cent of this clay, by weight, is coarser than the No. 200 sieve (0.074 mm). The specimen barely had enough cohesion to stand unsupported and be trimmed into a triaxial specimen.

CFS-Coordinates

Experimental Results

The results are presented in the form of diagrams of the variation of the defined cohesion and friction parameters with axial compressive strain. This set of coordinates will be referred to as the CFS-coordinates.

Figs. 16, 17, 18, 19, and 20 present the data for the extruded specimens. To avoid unnecessary confusion in these figures only the resulting curves are plotted without presenting the detailed data on which the curves are based. Some of this detail was presented previously in Fig. 6.

Because of possible special interest in the undisturbed specimen tests, and their comparatively limited number, the individual test data are presented for these tests. Along with each CFS-coordinate figure is presented the associated stress-strain curves so that the reader may see the test results in this more conventional form and, if desired, may compute the CFS-coordinate points. The above figures are numbered 21 through 24.

Discussion

Strain-Rate of Development of c and ϕ.—One of the most interesting and consistent observations made in this research is that the cohesion strength component generally develops to its maximum value at an axial compressive strain of less than 1 per cent, while the friction component requires a much greater strain to reach its maximum value. Since this observation can be made from the undisturbed as well as the extruded specimen test results, and is true for the considerable range of clay mineralogy and structure tested, it seems reasonable to conclude that this behavior is characteristic of many cohesive soils.

There seems to be a fundamental difference between the mechanical behavior of cohesion and friction in clay. These two strength components seem mechanically independent and this experimental observation suggests that the cohesion and friction definitions used herein may be fundamental in a mechanical sense.

On reflection, the above seems a reasonable behavior to expect since the cohesion is generally thought to be based on the electrical attractive forces between clay particles and large strains should not be required to activate these forces. On the other hand, friction is thought to depend on the interference between particles (6) and it is easier to imagine that considerable strain is required to achieve maximum interference and therefore maximum friction.

Cohesion Peak.—Not only does the cohesion component of strength develop very rapidly, but with some clays the cohesion reaches a maximum and then measurably decreases at a decreasing rate. The writers have named this maximum the "peak cohesion" and this behavior the "peaking effect." The magnitude of the peaking effect varies with the clay. It is essentially absent in the EPK, U-M, and U-LC clays (Figs. 13, 16, 17, 21, 22), moderate in the BBC clays (Figs. 18, 19, 23), and pronounced in the JSC and U-EPK clays

(Figs. 20, 24). If the peaking effect is measured as the ratio of (c_{peak}/c_{max} total strength, when $\bar{\sigma}_1 = \bar{\sigma}_{pct}$), the same clay at different void ratios has about the same "peaking ratio."

A possible, though at this time (Feb. 1960) tentative, explanation involves the amount of coarse grains in the cohesive soil. The EPK and U-M soils are almost pure clay, the BBC specimens have a considerable amount of silt since no attempt was made to separate the more silty layers, the JSC has a

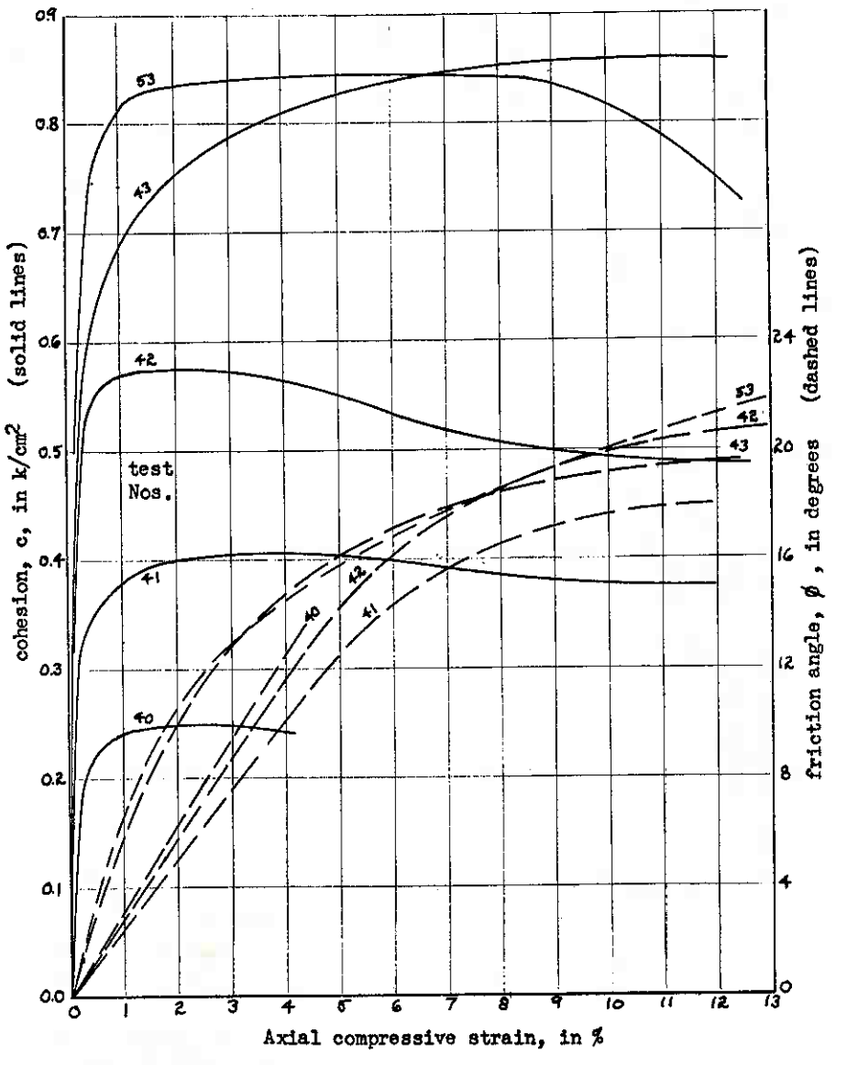

Fig. 16.—Computed Results CFS-Tests, DWEPK Samples

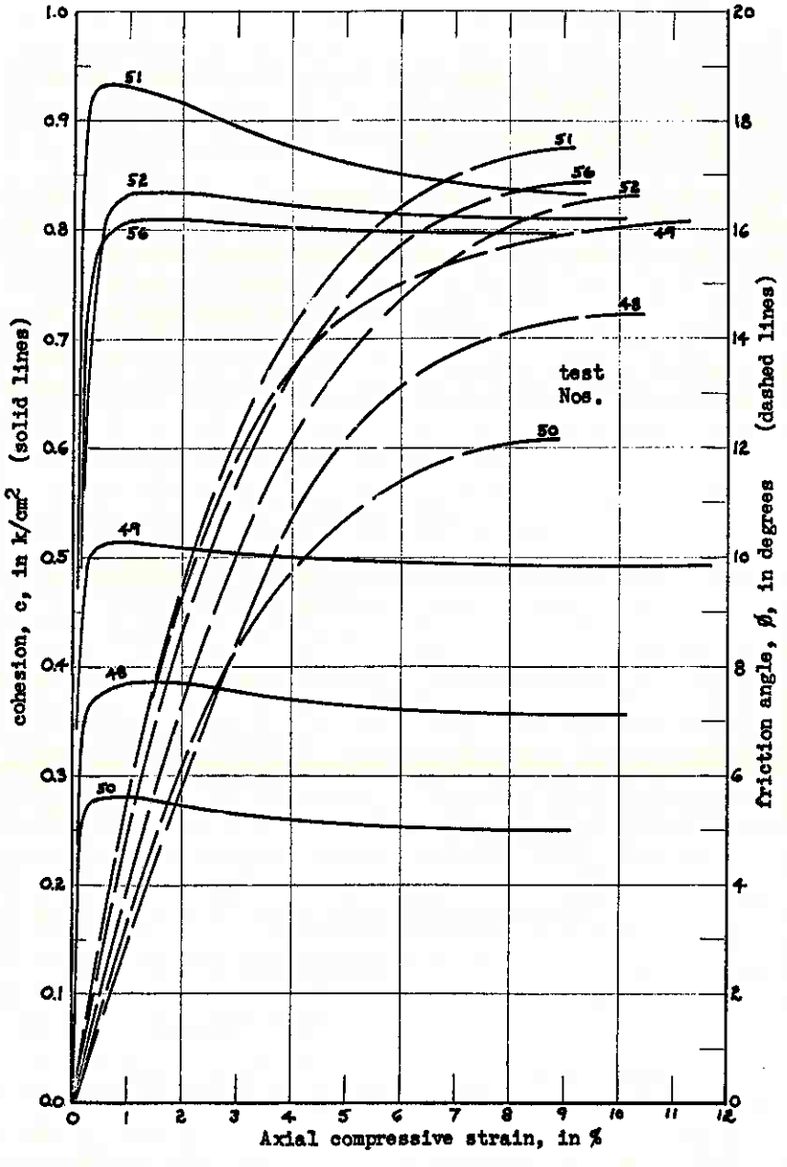

Fig. 17.—Computed Results CFS-Tests, N-EPK Samples

large amount of fine sand, and the U-EPK is mostly sand. It may be that the percentage of coarse grains in the soil, as well as the clay mineralogy, has an important influence on the development of a pronounced peaking effect. If true, this may be an important consideration in the cohesion behavior of compacted soils. The peaking effect may also depend on time parameters, such as rate-of-strain. However interesting such possibilities are, further investigation is certainly needed.

The existence of a pronounced peaking effect may lead to somewhat unexpected physical behavior. For instance, the JSC showed a surprisingly high compressibility for its low void ratio and PI. An example is test No. 77 where a saturated specimen with an initial void ratio of 0.674 consolidated to a void ratio of 0.560 with a hydrostatic consolidation pressure of only 1.17 kg/cm^2. Also, a clay with a pronounced peaking effect may exhibit a noticeable yield point in the stress-strain curve. This behavior occurs when the cohesion passes its peak and decreases more rapidly than the friction component is increasing, with the result of a temporary break in the constant $\breve{\sigma}_1$, stress-strain curves.

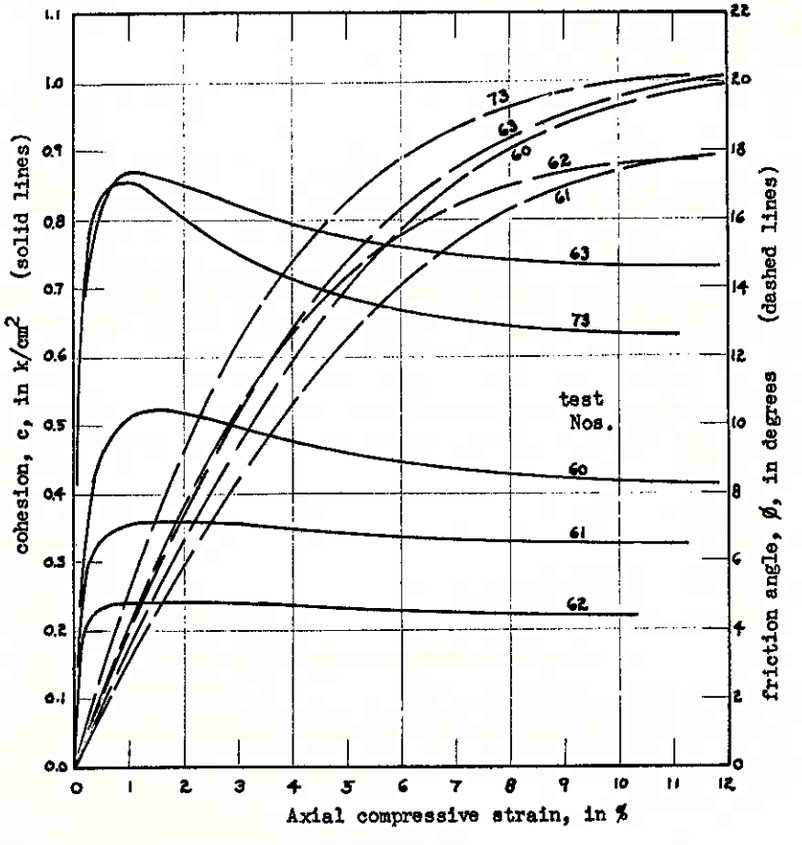

Fig. 18.—Computed Results CFS-Tests, BBC Samples

Friction.--Rosenqvist has presented a particularly clear explanation of the causes of friction within a clay soil (6). It is due primarily to the macro and micro-dilatency of the particle structure, or in the simple view, just particle interference. At decreasing void ratio, the particles are packed closer together and one would therefore expect particle interference, and therefore ϕ to increase. On the other hand, consolidation also tends to orient the particles to a more parallel arrangement and such a change might reduce particle interference and therefore reduce ϕ. Thus, one can visualize these two opposing tendencies in action and ϕ may go either way or remain the same during consolidation.

The tests on kaolinite indicated a reduction in ϕ as particle parallelism was increased with the sodium di-phosphate deflocculant--in spite of the greatly reduced void ratio. The average maximum friction angle was about

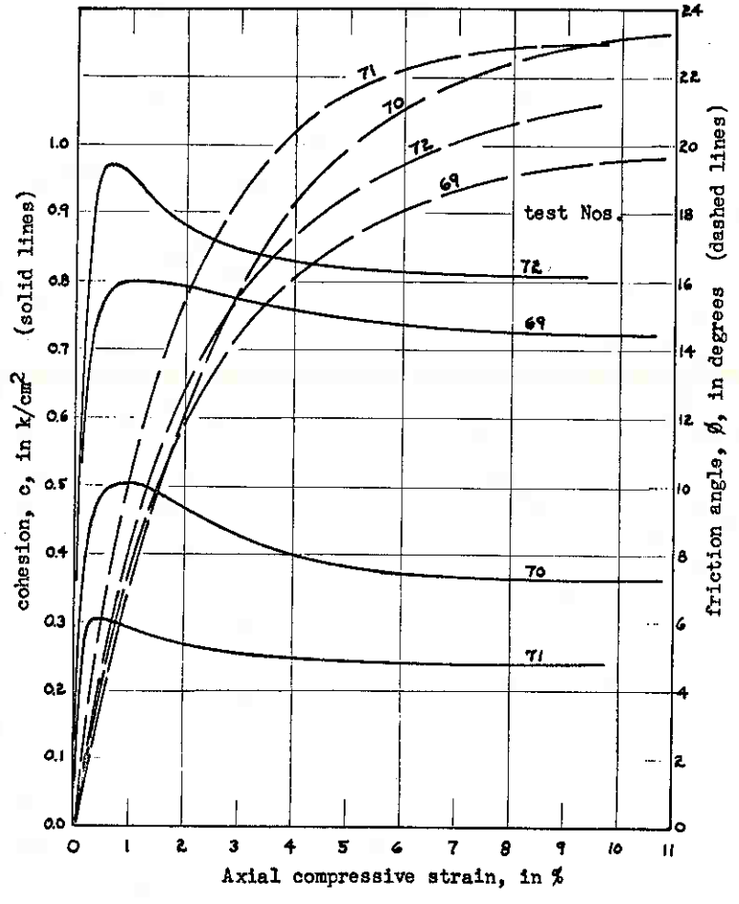

Fig. 19.--Computed Results CFS-Tests, Q-BBC Samples

20 degrees for DWEPK and 16 degrees for N-EPK. On the other hand, the reduction of void ratio of the N-EPK by hydrostatic consolidation steadily increased ϕ (Fig. 17).

The BBC had a ϕ range of about 18-20 degrees, while the Q-BBC ranged from 20-23 degrees. For this soil it appears that the reduction in void ratio and its effect of increasing ϕ overshadowed the decreasing effect of more particle parallelism. There seemed to be no consistent tendency for either BBC soil to increase ϕ with consolidation. The same appears true for the JSC specimens. However, it should be remembered that these tests were all

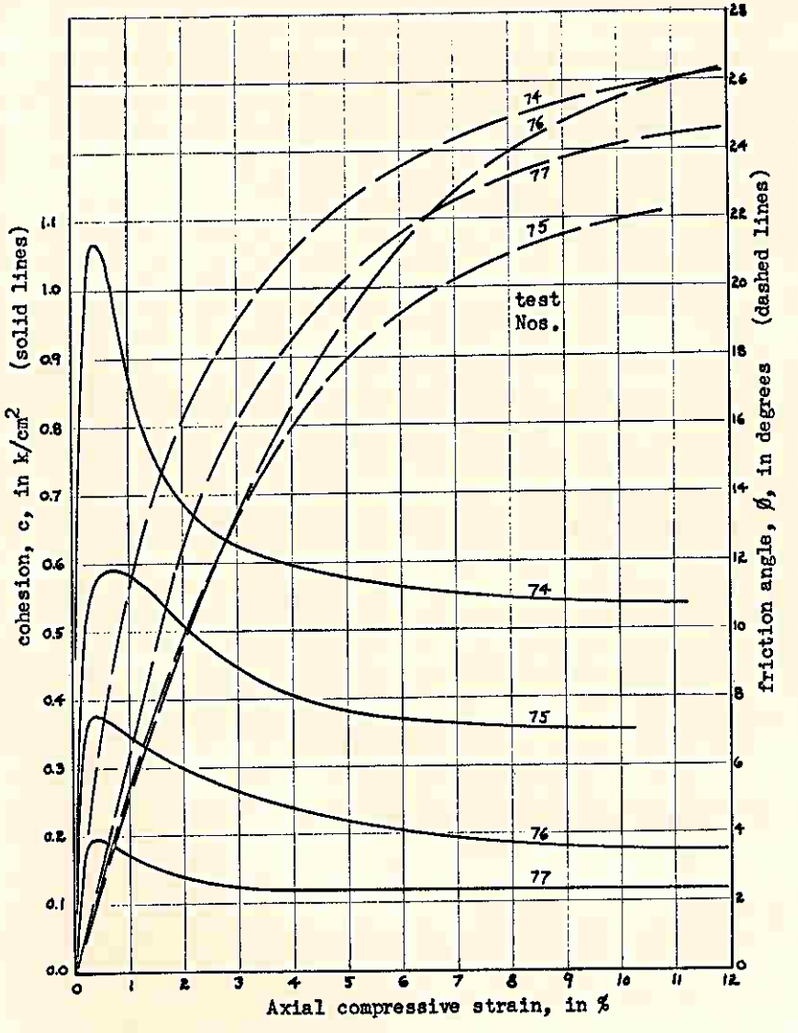

Fig. 20.--Computed Results CFS-Tests, JSC Samples

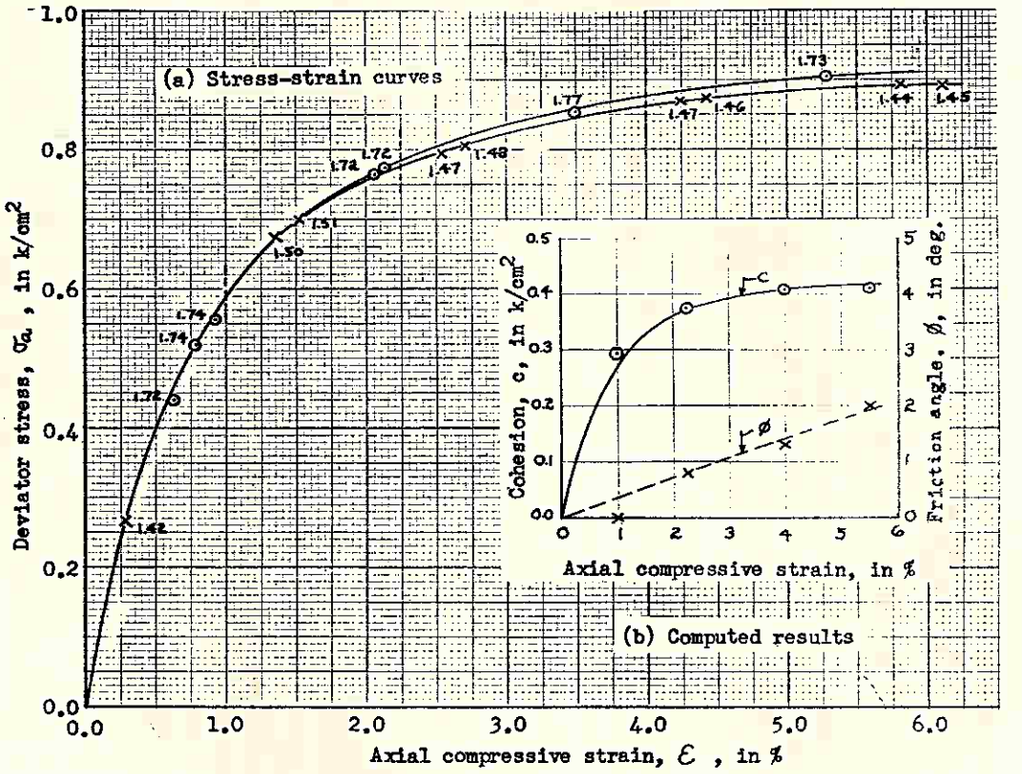

Fig. 21.—CFS-Test No. 88, Sample U-LC 3R/7

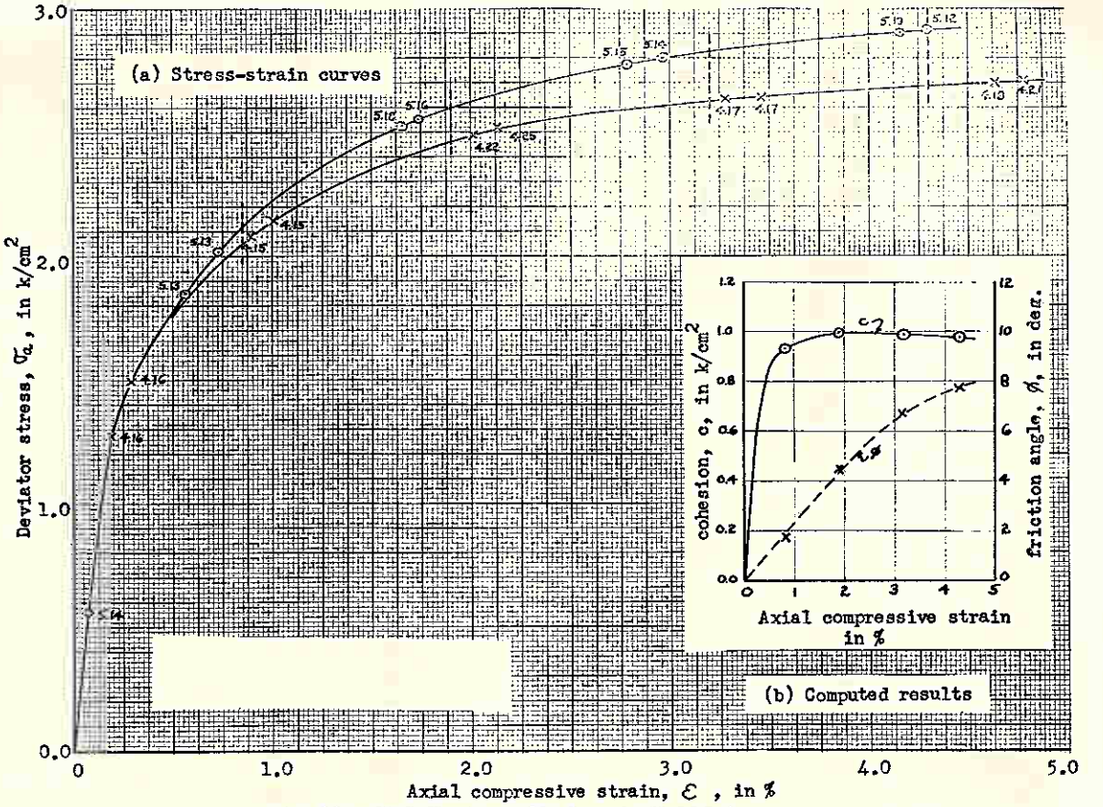

Fig. 22.—CFS-Test No. 89, Sample U-M I-1

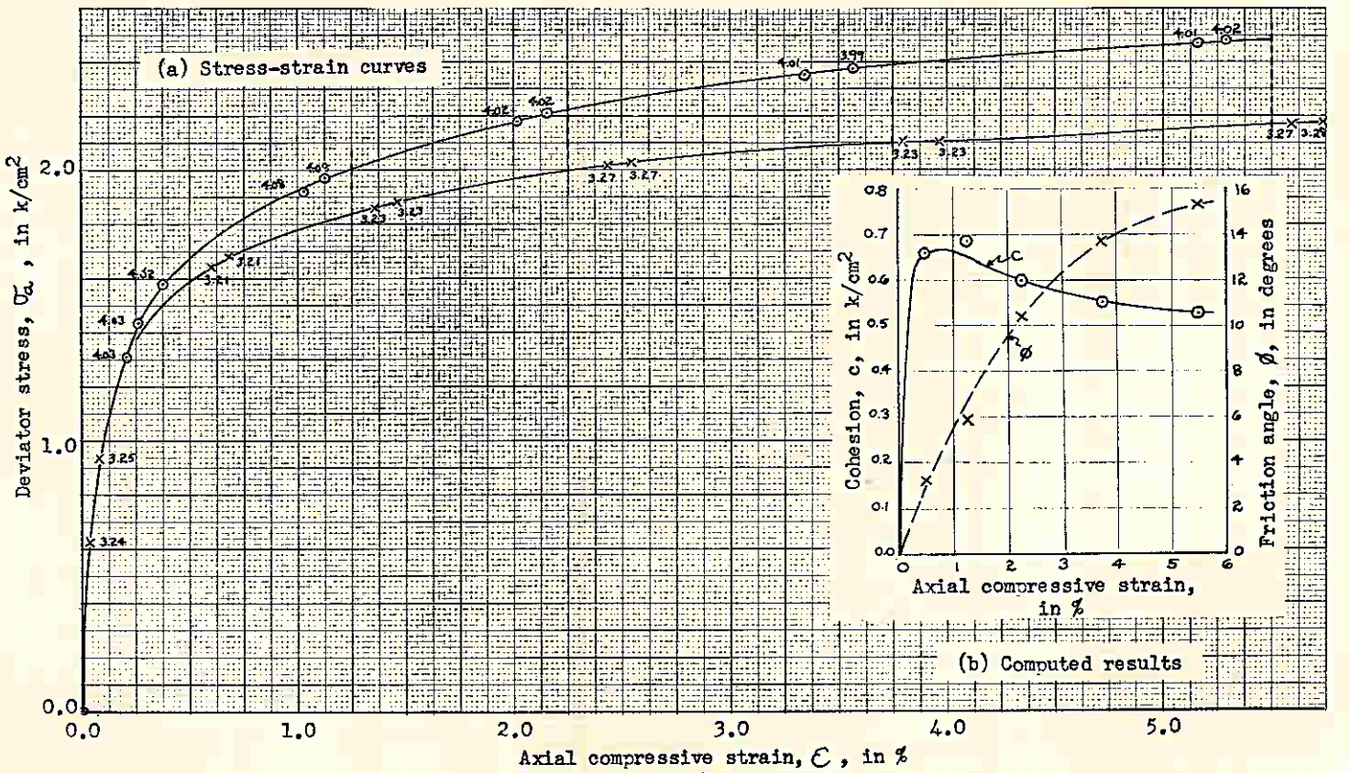

Fig. 23.—CFS-Test No. 91, Sample U-BBC 4

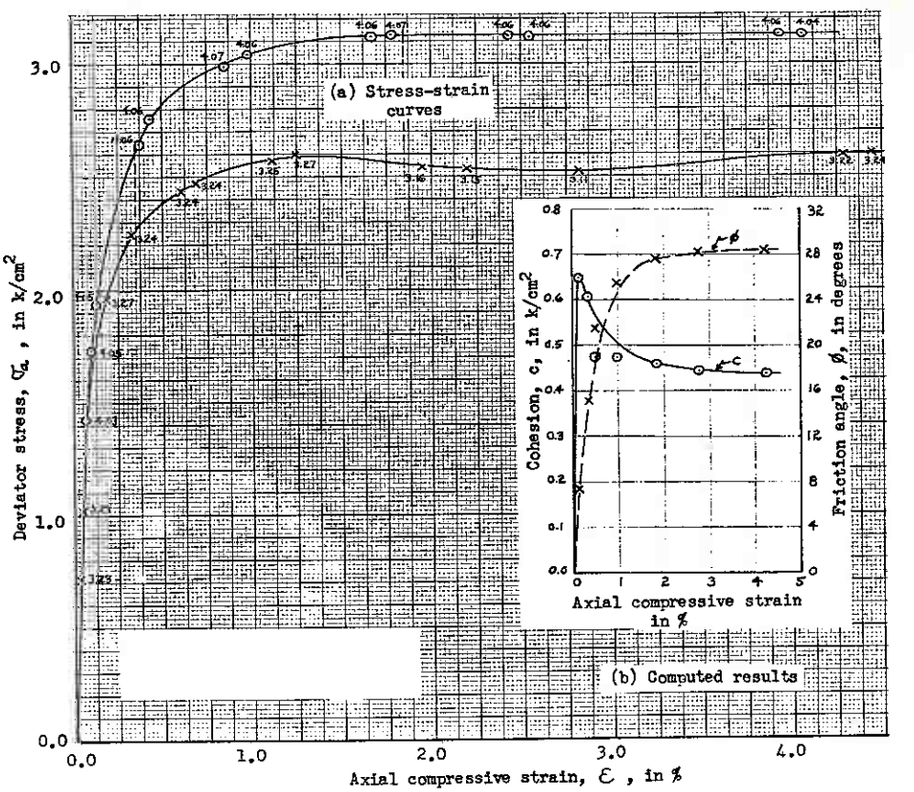

Fig. 24.—CFS-Test No. 92, Sample U-EPK

done using the stage 2 technique and the results might have been more definitive had the more accurate stage 3 technique been used.

It has been suggested that the angle of inclination of the failure plane with the horizontal in a compression test performed with increasing stress on a horizontal plane is related to ϕ by the equation $\alpha = 45^0 + \frac{\phi}{2}$ where α is the angle of inclination. Bjerrum reports a statistical correlation using unconfined tests (3). It is therefore of some interest to compare the CFS-test determined values of internal friction with the values computed from failure plane angles measured in those tests where failure planes were noted and measured at the end of the test.

Comparison of the CFS-test results with measured failure plane angles is indicated in Table IV.

Table IV

Test No.	Soil	Friction angle ϕ, in degrees	
		CFS-Test	Computed from α
41	DEWPK	18	26
42	DWEPK	21	20
43	DEWPK	20	24
49	N-EPK	16	26
50	N-EPK	12	20
51	N-EPK	18	24
52	N-EPK	17	22
56	N-EPK	17	30
69	Q-BBC	20	24
70	Q-BBC	23	30
80	U-M	12	16
87	U-M	11	20

From these results it appears that only a poor correlation exists between the two methods. The CFS-test method of computing ϕ may have unsuspected errors. Or, the helical structure imposed by extrusion may have prejudiced the failure plane angle. But, it is also possible, for instance, that the neglected existence of shear forces on the loading caps during the development of the failure plane may account for an inaccuracy in the α method of computing ϕ.

Coulomb-Hvorslev Coordinates

The results from the extruded specimen test series are also presented in the form of Mohr circles, using shear stress for the ordinate and intergranular normal stress for the abscissa. Since the envelope to a series of Mohr circles defines a line whose linear approximation is known as the Coulomb equation, and the importance of using intergranular stress was one of the results of Hvorslev's work (1), these coordinates are herein referred to as the Coulomb-Hvorslev coordinates.

Five plots, one for each series of extruded specimens, are presented in Figs. 25 to 27. In general the circles plotted represent the maximum compressive strength of the specimen at the particular value $\bar{\sigma}_1 = \bar{\sigma}_{pct}$. Where

this is not the case it is noted on the figure. It is also of interest that the maximum deviator stress and maximum stress ratio criteria of failure are identical in tests performed at constant $\bar{\sigma}_1$.

It may be noted in the above figures that the envelopes plot in the conventional manner. The fact that the envelopes do not pass directly through the origin of coordinates may be due to a combination of extrusion preconsolidation, the effects of the membranes--for which no correction was attempted, and the net effect of using internal and external drains--also for which no correction was attempted.

The angle of inclination of the envelope to the circles is herein called β. Comparison of the β angles with the CFS-test determined angles of internal

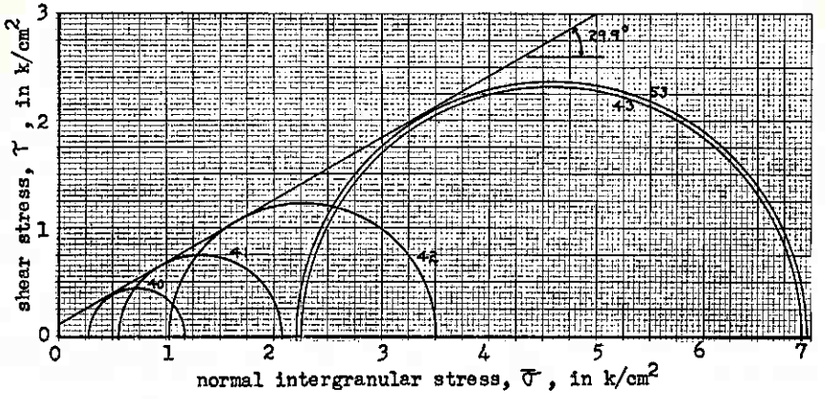

(a) DWEPK Samples

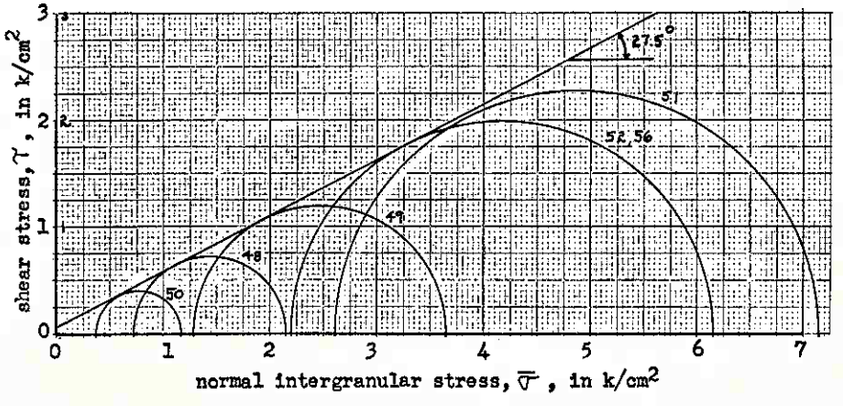

(b) N-EPK Samples

Fig. 25.—Summary of Results

friction show poor agreement, with β generally 6 to 12 degrees greater than the average ϕ. β could be defined as the angle whose tangent is the rate of strength increase with normal consolidation. Since this increase is at least partly due to an increase in the cohesion component of strength, β should not be compared with the ϕ defined herein.

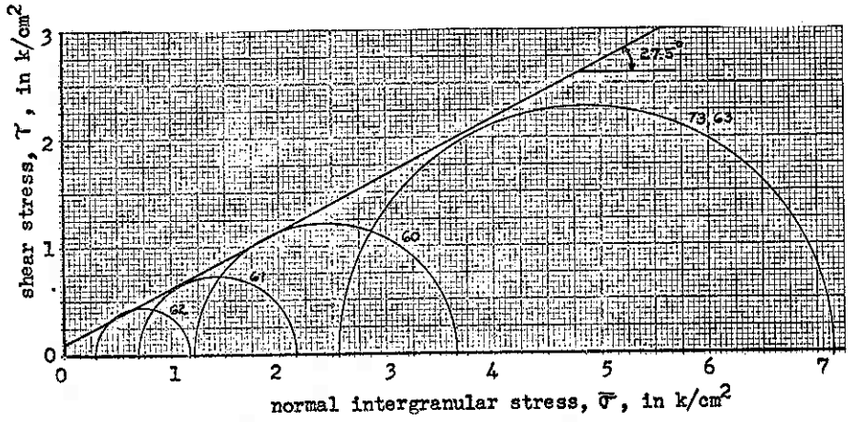

(a) BBC Samples

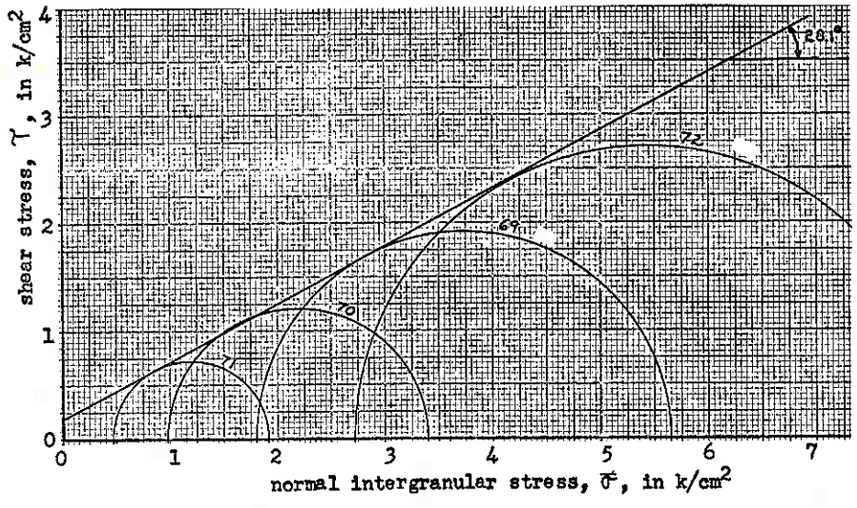

(b) Q-BBC Samples

Fig. 26.—Summary of Results

Rutledge Coordinates

Experimental Data

Another potentially instructive way of presenting the experimental data is by plotting void ratio (or water content) as the ordinate and both strength and consolidation pressure (log scale) as the abscissa. These coordinates will herein be referred to as the Rutledge coordinates.

The five series of tests on extruded specimens are presented on Figs. 28 to 30. Plotted as abscissa are the hydrostatic preconsolidation pressure, the value of the compressive strength—the same as the diameters of the Mohr circles shown in Figs. 25 to 27, and twice the value of the peak cohesion. Twice the peak cohesion is chosen to give a direct picture of the total compressive strength that could be developed by cohesion alone, although this strength does not occur at the same strain as the maximum total strength of the specimen.

In addition to the above, the Rutledge coordinate plots were taken as a basis for interpolation of results at selected values of preconsolidation pressure. These interpolated results are presented in Table V.

Discussion

Parallelism of Compressive Strength and Consolidation Curves.—The Rutledge coordinate plots show the expected parallel relationship between the void ratio-consolidation and the void ratio-compressive strength curves. This parallelism has been demonstrated many times since Rutledge discussed it (3, 14). As reviewed below, this relationship of a constant ratio between consolidation pressure and strength must be so if the Coulomb-Hvorslev coordinate plots yield envelopes that are straight lines passing through the origin. If β is the constant angle of inclination of this line, and $\bar{\sigma}_1 = \bar{\sigma}_{pct}$,

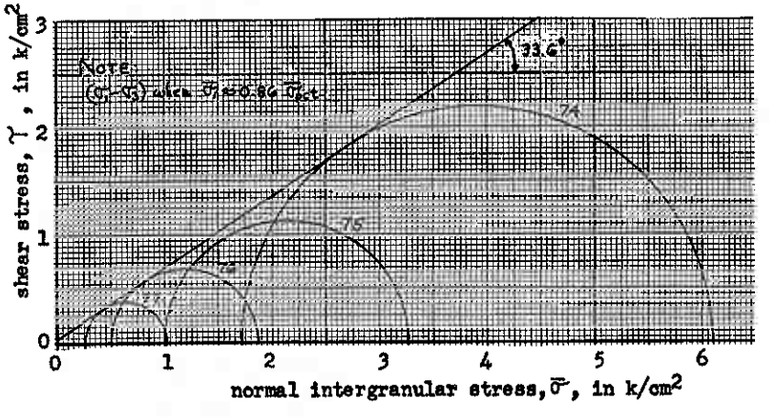

Fig. 27.—Summary of Results, JSC Samples

then: $\frac{\bar{\sigma}_{pct}}{(\sigma_1 - \sigma_3)} = \frac{\sin \beta + 1}{2 \sin \beta}$, which is constant for constant β.

Variation of Cohesion with Void Ratio.—Reference to Figs. 28 to 30, 16 to 20, shows that the CFS-test measured peak cohesion, and also the cohesion at any particular strain if such was chosen for plotting, increases logarithmically as void ratio decreases linearly. This agrees with the results reported by Bjerrum (3).

From the results of the work by Hvorslev (1), it is normally assumed that the cohesion varies with water content. That is, at the same water content a certain clay has a constant cohesion. What was perhaps sometimes previously not sufficiently appreciated, and is clearly demonstrated by this research, is the great importance of soil structure in determining cohesion.

At the same void ratio the cohesion of a clay can vary many fold—for example, as is shown by the cohesion differences between DWEPK and N-EPK at e = 0.830 (Fig. 28), and between BBC and Q-BBC when the cohesion values are extrapolated to e = 0.580 (Fig. 29). It may be argued that the chemical additives used here have altered the clay and the above are not comparisons for the same clay. This may be true to some extent, but the writers believe that the same observations could be made on any comparison of cohesion, as measured in the CFS-test, for any structurally sensitive clay at constant void ratio and chemical content but at different stages of structural disturbance. The comparison of test No. 91 on U-BBC with the BBC series supports this opinion, though it would be more convincing if these specimens had been obtained from the same test pit sample.

It seems clear that both void ratio (water content) and structure must be specified when evaluating or comparing cohesion. Since a given void ratio for a given clay at a given structure can only be attained for a certain consolidating pressure (neglecting secondary time effects associated with consolidation), it is possible that the consolidating pressure is a more fundamental variable to consider.

Variation of Cohesion with Consolidation Pressure.—Reference is now made to Table V wherein the peak cohesion values are compared at three values of hydrostatic consolidation pressure. In addition to the extruded specimen results presented in this table, the stage 3 results obtained from the undisturbed specimen tests are included.

It may thus be seen that in spite of the differences in mineralogy, grain size distribution, void ratio, and structure represented by the extruded and undisturbed specimens, the measured peak cohesion at a given hydrostatic preconsolidation pressure varies only 10 to 14 per cent from the average value at each pressure. Both Hvorslev (1) and Bjerrum (3) noted that the cohesion of a normally consolidated, remolded soil could be expressed as a constant times the "equivalent consolidation pressure," σ_e. The above experimental results indicate that the same constant, or near-constant, may apply to many cohesive soils. A possible explanation for this behavior is:

1. When a specimen is undergoing triaxial consolidation under hydrostatic pressure there are no shearing stresses within the specimen. However, this can only be true when one considers average stresses over relatively large areas within the specimen. Since the specimen is undergoing considerable volume change the clay mineral grains must be reorienting themselves within the soil to accommodate the change. Since the grains can be assumed incompressible, this reorientation is

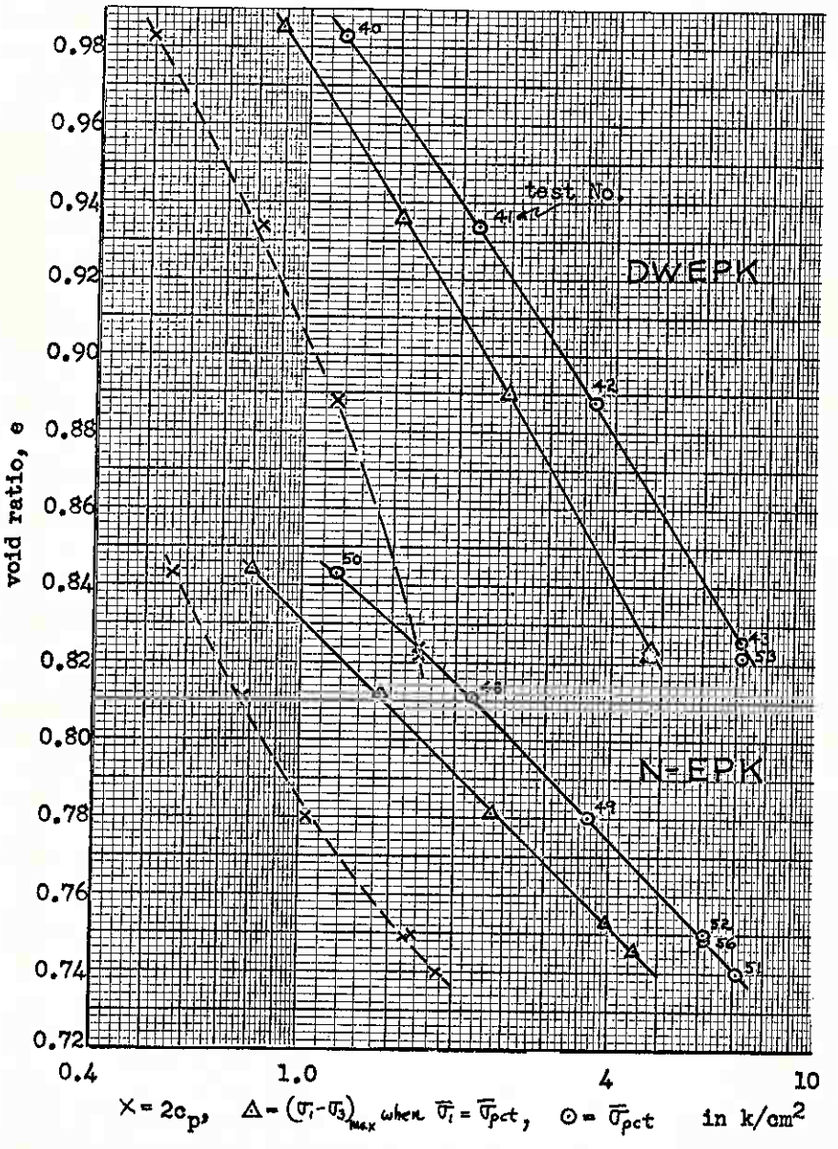

Fig. 28.—Summary of CFS-Tests on EPK

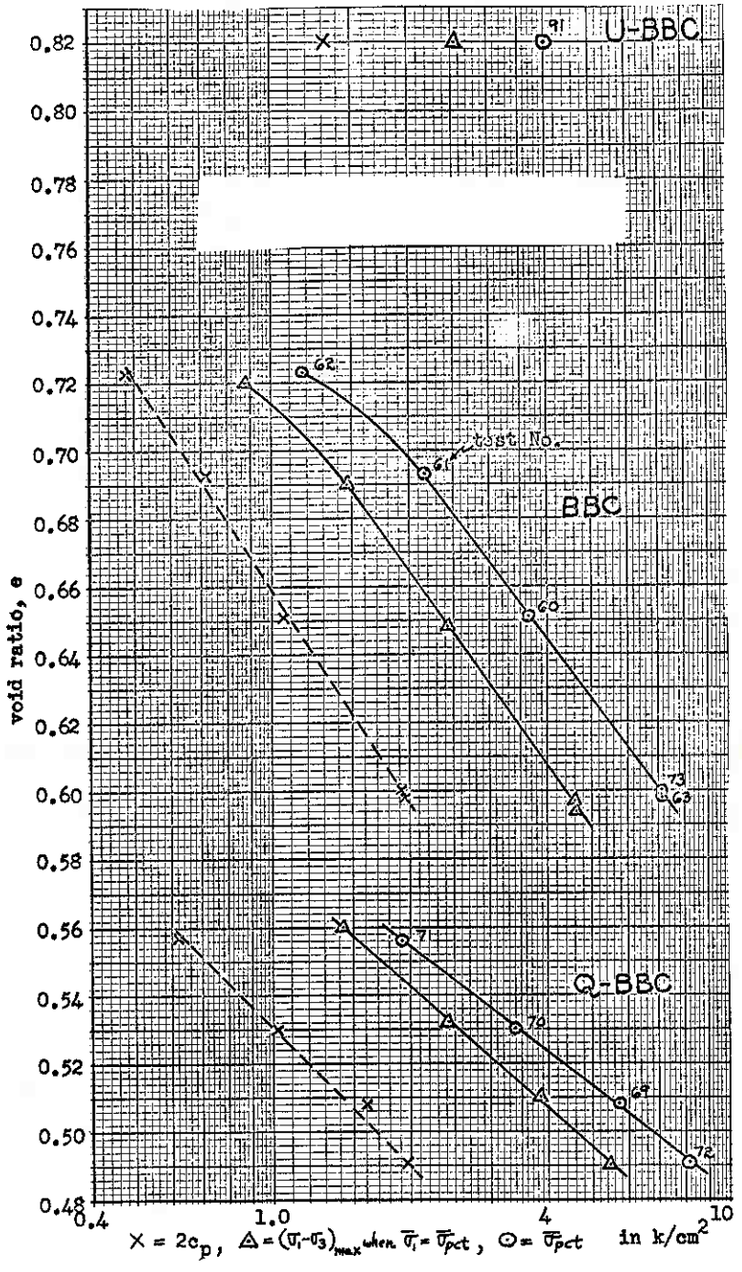

Fig. 29.—Summary of CFS-Tests on BBC

visualized as largely a slipping, or shearing action of a portion of one particle over its neighbor to reform the group into a denser structure. On the microscopic level there must be shear. However, with the generally small volume strains of consolidation the average shear strains are probably small.

2. It is the sum total of all of these microscopic shear stresses, together with any compressive stresses within the structural framework, that

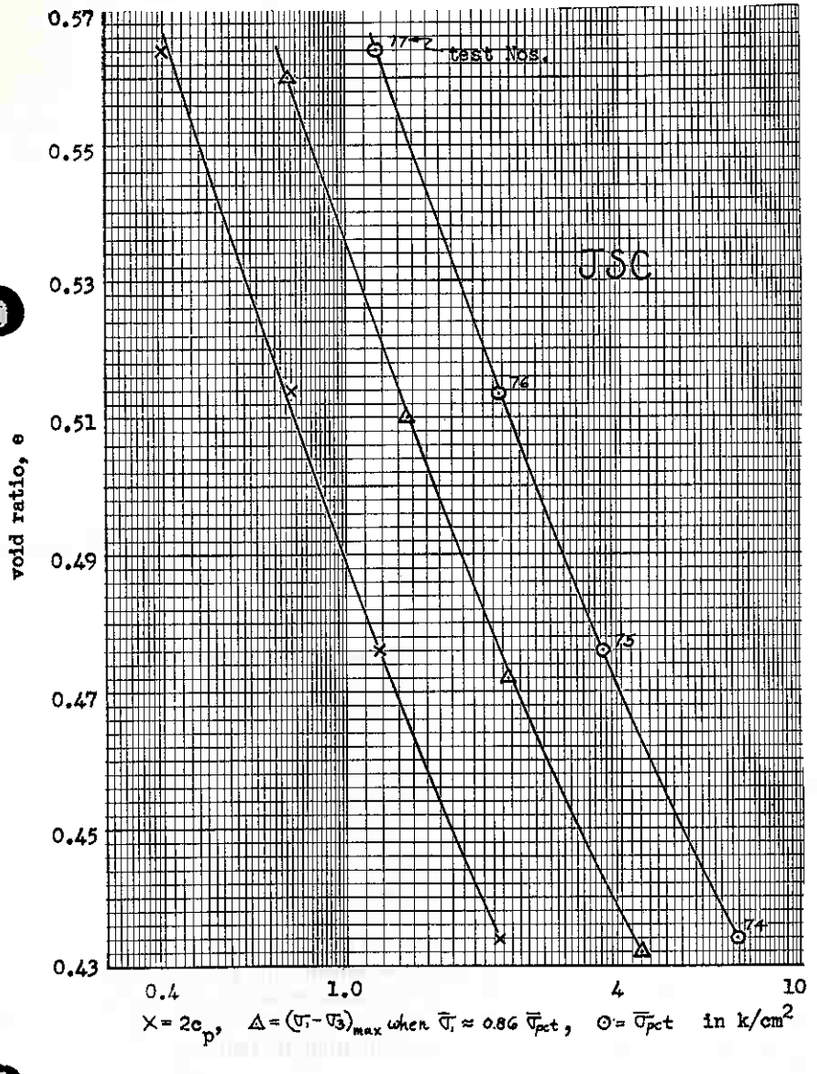

Fig. 30.--Summary of CFS-Tests on JSC Samples

Table V.—Peak Cohesion and Consolidation

1	2	3	4	5	6
$\bar{\sigma}_{pct}$(k/cm^2)	Clay	e	$2c_p$(k/cm^2)	$(2c_p/\bar{\sigma}_{pct})$%	Vol. Strain $\Delta e/(1+e_o)$
2.0	DWEPK	0.939	0.75	37.5	0.040
	N-EPK	0.815	0.73	36.5	0.021
	BBC	0.698	0.65	32.5	0.031
	Q-BBC	0.554	0.67	33.5	0.039
	JSC	0.520	0.68	34.0	0.093
	U-LC	1.45	0.82	41.0	0.303
4.0	DWEPK	0.879	1.23	30.7	0.070
	N-EPK	0.774	1.14	28.5	0.043
	BBC	0.645	1.17	29.2	0.061
	Q-BBC	0.523	1.12	28.0	0.058
	JSC	0.469	1.30	32.5	0.124
	U-BBC	0.820	1.36	34.0	0.074
	U-EPK	0.516	1.29	32.2	0.084
7.0	DWEPK	0.827	1.81	25.8	0.096
	N-EPK	0.741	1.82	26.0	0.061
	BBC	0.601	1.90	27.1	0.086
	Q-BBC	0.498	1.74	24.8	0.074
	JSC	0.435	2.12	30.3	0.144

combats the volume reducing effect of the preconsolidating load until the sample resistance to deformation, or its strength, increases and a new equilibrium is established at a reduced void ratio. The secondary creep phenomena is neglected here.

3. During consolidation the shear strains are small. This research has shown, with the clays tested, that at small strains the cohesion is the greatly predominant strength component. It would seem to follow then that the sample strength resisting the volume change of consolidation is predominantly, perhaps almost entirely, the cohesion.

If this reasoning is correct, then it is reasonable to expect that a certain preconsolidating pressure will reduce the void ratio of a clay until that value of cohesion is developed which can resist further volume change—thus the good experimental agreement between the preconsolidation pressure and the peak cohesion values in spite of the great differences in the other variables.

An observation that tends to support the above reasoning is the reduction in the $2c_p/\bar{\sigma}_{pct}$ ratio with increasing hydrostatic preconsolidation pressure, as shown in column 5 of Table V. The specimens were consolidated by one increment of pressure and the volume strain increased with the $\bar{\sigma}_{pct}$ value, as shown in column 6 of this table. With the increase in strain, more of the specimen friction is mobilized and it is no longer necessary to develop the same proportion of cohesion to resist the consolidating pressure, with the result that the $2c_p/\bar{\sigma}_{pct}$ ratio decreases.

V. CONCLUSIONS

1. A laboratory triaxial test for saturated clays has been developed that permits the measurement of cohesion and friction, defined in terms of the empirical definition of intergranular stress on the plane of maximum stress obliquity for the frictional component of strength, at strain intervals over the range of testing. This test, herein called the CFS-test, has the advantages of being practical, accurate, and applicable to all soils investigated to date (Feb. 1960). In addition, only a single specimen is required and therefore undisturbed specimens can be tested. A disadvantage is that triaxial equipment of the quality required is presently available in only comparatively few laboratories, but this disadvantage should be only temporary.

2. The Coulomb-Hvorslev equation, previously known to be valid for the failure condition, is shown to be valid over the entire strain and $(\bar{\sigma}_1/\bar{\sigma}_{pct})$ range of testing used in this research.

3. It has been shown that the defined cohesion component of strength develops to its maximum value at small axial compression strains, while the frictional component of strength usually requires much larger strains to develop. Cohesion is at its maximum while the friction is often negligible at the strain of maximum cohesion. The two defined strength components appear to be mechanically independent.

4. It has been demonstrated that some clays rapidly reach their maximum cohesion value and this value then decreases with continued strain while the friction continues to increase. This behavior has been termed the "peaking effect" and the maximum value of cohesion is termed the "peak cohesion." It seems likely that the peaking effect is increased as the amount of coarse particles in the clay is increased.

5. It has been shown that the peak cohesion is primarily dependent on the hydrostatic preconsolidating pressure $\bar{\sigma}_{pct}$. At constant $\bar{\sigma}_{pct}$ it is dependent to a much lesser degree on the variables of void ratio, structure, mineralogy, and grain size distribution. The experimental evidence also indicates that the greater the volume strain during the consolidation increment, the smaller the proportional value of the specimen cohesion. A qualitative theory is proposed to account for this behavior.

This work reports the results of a primarily exploratory, research investigation of the cohesion-friction-strain behavior of cohesive soils. Some potentially important complications in this behavior do not fall within the scope of this paper—for instance, the effects of different rate-of-strain on the cohesion-friction distribution, and also an evaluation of the long-time stability of the cohesion and friction components at both constant strain and constant stress. Still other factors not investigated herein and which should be studied with the CFS-test technique are: The effects of anisotropical and one-dimensional consolidation on the cohesion and friction components, cohesion and friction behavior at very small and very large axial strains, effect of overconsolidation, swelling clays, partially saturated clays, and thixotropic clays.

ACKNOWLEDGMENTS

This work was performed in the Soil Mechanics Research Laboratory of the University of Florida by the senior author as part of a Ph.D. thesis to be

submitted to Northwestern University. The work was under the direction of the junior author.

This research was sponsored by the National Science Foundation, grant Nos. G-4636 and G-10827, and by the Engineering and Industrial Experiment Station of the University of Florida, project No. 5769. These agencies are thanked for making this work financially possible.

Dr. F. E. Richart, Jr., Professor of Civil Engineering at the University of Florida, Gainesville, Florida, is thanked for his helpful suggestions and general interest in this work. Mr. John R. Hall, Jr., graduate research assistant in the University of Florida Soil Mechanics Research Laboratory, assisted the senior author in the development of the stage 3 technique.

The writers' appreciation is also extended to the following, who contributed some of the soil samples used in this research: Mr. Robert Crisp, Jr., Chief, Soil Mechanics Branch, South Atlantic Division Lab., U. S. Army Corps of Engineers, Marietta, Ga.; Mr. Allen Edgar of the Edgar Plastic Kaolin Co., Edgar, Fla.; Eustis Engineering Co., Metairie, La.; Mr. Blase McCarthy, Instructor of Civil Engineering, University of Florida; Dr. F. E. Richart, Jr.; and Mr. Paul H. Shea, Chief, Foundations and Materials Branch, U. S. Army, Engineer District, Jacksonville, Fla.

A note of acknowledgment is also extended the Norwegian Geotechnical Institute and GEONOR A/S, both of Oslo, Norway, for the excellent triaxial testing equipment they helped develop and now manufacture. The availability of this equipment greatly aided this research.

APPENDIX I.—NOTATIONS

c = cohesion, as defined in this paper

$\bar{c}$ = effective cohesion

c_p = peak cohesion

c_ϵ = cohesion at strain ϵ

e = void ratio

e_o = void ratio before consolidation

s_o = degree of saturation before consolidation

u = pore water pressure, as measured by a piezometer

α = angle of failure plane with horizontal in an axial compression test

β = angle of Mohr failure envelope with $\bar{\sigma}$ axis

ϵ = axial compressive strain

σ = normal stress

$\bar{\sigma}$ = normal intergranular stress

σ_h = triaxial cell pressure

σ_1 = major principal stress

$\bar{\sigma}_1$ = major principal intergranular stress

σ_3 = minor principal stress

$\bar{\sigma}_3$ = minor principal intergranular stress

σ_a = $(\sigma_1 - \sigma_3)$ = deviator stress, applied axially by piston

σ_e = equivalent consolidation pressure, equals pressure on virgin consolidation curve at same void ratio as sample

$\bar{\sigma}_{pct}$ = hydrostatic, triaxial preconsolidation pressure

$\bar{\sigma}_\phi$ = normal intergranular stress on the plane of maximum stress obliquity of the frictional component of strength

τ = shear stress

τ_ϕ = shear stress on the plane of maximum stress obliquity of the frictional component of strength

ϕ = angle of internal friction as defined in this paper

$\bar{\phi}$ = effective angle of internal friction

ϕ_ϵ = angle of internal friction at strain ϵ

APPENDIX II.—REFERENCES

1. "Über die Festigkeitseigenschaften Gestörter Bindiger Böden," by M. Juul Hvorslev, Ingeniørvidenskabelige Skrifter, A Nr. 45, Danmarks Naturvidenskabelige Samfund, København, 1937.
2. "Cooperative Triaxial Shear Research Program of the Corps of Engineers," review prepared by Philip C. Rutledge, Soil Mechanics Fact Finding Survey, Progress Report, Waterways Experiment Station, Vicksburg, Mississippi, April, 1947.
3. "Theoretical and Experimental Investigations on the Shear Strength of Soils," by L. Bjerrum, Norwegian Geotechnical Institute publication No. 5, Oslo, 1954.
4. "The Pore Water Coefficients A and B," by A. W. Skempton, Geotechnique, Vol. 4, No. 4, December, 1954.
5. "The Engineering Behavior of Compacted Clay," by T. William Lambe, Journal of the SM and F Div., ASCE, paper 1655, May, 1958.
6. "Physico-Chemical Properties of Soils: Soil-Water Systems," by I. Th. Rosenqvist, Journal of the SM and F Div., ASCE, paper 2000, April, 1959.
7. "The Role of Effective Stress in the Behavior of Expansive Soils," by T. William Lambe and Robert V. Whitman, Soil Engineering Division, Massachusetts Institute of Technology, April, 1959.
8. "Triaxial Equipment Developed at the Norwegian Geotechnical Institute," by A. Andresen, L. Bjerrum, E. DiBiago and B. Kjaernsli, Norwegian Geotechnical Institute publication No. 21, Oslo, 1957.
9. "Prestress Induced in Consolidated-Quick Triaxial Tests," by A. Casagrande and S. D. Wilson, Proceedings of the 3rd Int. Conf. on SM and FE, Switzerland, 1953, Vol. 1, p. 106.

10. "De-Aired, Extruded Soil Specimens for Research and for Evaluation of Test Procedures," by H. Matlock, Jr., C. W. Fenske and Raymond F. Dawson, ASTM Bulletin No. 177, October, 1951.

11. The Measurement of Soil Properties in the Triaxial Test, by Bishop and Henkel, Edward Arnold Ltd., London, 1957.

12. "Fundamental Factors Affecting the Deformation Behavior of Clay-Water Systems. I. Raw Material Studies," by C. W. Ormsby, Nat. Bur. of Stds. Report No. 5658, U. S. Dept. of Commerce, Washington, D. C., November, 1957.

13. "Effect of Structure on the Secondary Compression of Kaolinite," by James W. MacFarlane, unpublished master's thesis, Univ. of Florida, January, 1959.

14. "Effect of Sample Disturbance on the Strength of a Clay," by Max L. Calhoon, Transactions, ASCE, Vol. 121, 1956, p. 925.

PUBLICATIONS OF THE FLORIDA

ENGINEERING AND INDUSTRIAL EXPERIMENT STATION

The Engineering and Industrial Experiment Station, College of Engineering, issues five series of publications under the general title, *ENGINEERING PROGRESS at the University of Florida:* (1) Bulletin Series – original publications of research, or conference proceedings, usually on problems of specific interest to the industries of the State of Florida; (2) Technical Paper Series – reprints of technical articles by staff members appearing in national publications; (3) Leaflet Series – nontechnical articles of a general nature written by staff members; (4) Technical Progress Reports – reports of research which is still in progress, and (5) Florida Engineering Series – books on technical engineering problems.

A complete list of these publications is available upon request to:

The Editor
Florida Engineering and Industrial Experiment Station
University of Florida
Gainesville, Florida